UPPSALA
UNIVERSITET

Digital Comprehensive Summaries of Uppsala Dissertations from the Faculty of Science and Technology 1236

Ab initio Studies on Exchange Interactions in Metals and Correlated Oxides

ADAM JAKOBSSON

ACTA
UNIVERSITATIS
UPSALIENSIS
UPPSALA
2015

ISSN 1651-6214
ISBN 978-91-554-9190-1
urn:nbn:se:uu:diva-246766

Dissertation presented at Uppsala University to be publicly examined in room 10132, Ångströmslaboratoriet, Lägerhyddsvägen 1, Uppsala, Friday, 17 April 2015 at 10:00 for the degree of Doctor of Philosophy. The examination will be conducted in English. Faculty examiner: Nicola Spaldin (Swiss Federal Institute of Technology (ETH) Zurich).

Abstract
Jakobsson, A. 2015. Ab initio Studies on Exchange Interactions in Metals and Correlated Oxides. *Digital Comprehensive Summaries of Uppsala Dissertations from the Faculty of Science and Technology* 1236. 53 pp. Uppsala: Acta Universitatis Upsaliensis.
ISBN 978-91-554-9190-1.

A report is given on the implementation of a frozen magnon technique in the FLAPW code FLEUR, showing that the procedure reduced computational costs compared with a previously implemented method, while delivering accurate results. Furthermore a generalisation was made of the well known one lattice formula that connects the total energy differences of spin-spirals to the adiabatic magnon excitation energies to multiple lattice systems.

The implemented method was applied to B2 structured FeCo to investigate the changes of the Curie temperature with a tetragonal distortion and it was found that the FeCo films grown on Rh have characteristics that makes it a good candidate for HAMR storage media. The method was also applied to a selection of spin-gapless semiconductors in order to investigate their magnetic properties. It was found that all of the studied materials have a Curie temperature well above room temperature and excellent agreement with experimental results was obtained for the material Mn_2CoAl that has been synthesised.

Finally, the implemented frozen magnon method was adjusted to include constraining fields to restrict the directions of the magnetic moments. It was shown that this procedure significantly improved the agreement between the dispersion for all considered spin-spiral configuration and introduced significant adjustments of the exchange parameters. However for other materials, such as bcc-Fe, such corrections yield worse results and, motivated by the need for a consistent method, we considered a self consistent spin-spiral based method to extract the exchange parameters from the inverse transverse static magnetic susceptibility. Preliminary results show that the newly implemented method gives results close to the corrected frozen magnon method for FeCo and results close to the uncorrected frozen magnon method for bcc Fe and thus provides a consistent improvement over the two previously used methods.

Adam Jakobsson, Department of Physics and Astronomy, Materials Theory, Box 516, Uppsala University, SE-751 20 Uppsala, Sweden.

ISSN 1651-6214
ISBN 978-91-554-9190-1
urn:nbn:se:uu:diva-246766 (http://urn.kb.se/resolve?urn=urn:nbn:se:uu:diva-246766)

To Corina

List of papers

This thesis is based on the following papers, which are referred to in the text by their Roman numerals.

I **Exchange parameters and adiabatic magnon energies from spin-spiral calculations**
Adam Jakobsson, Biplab Sanyal, Marjana Ležaić, and Stefan Blügel
Phys. Rev. B 88, 134427 (2013)

II **Tuning the Curie temperature of FeCo compounds by tetragonal distortion**
A. Jakobsson, E. Şaşioğlu, Ph. Mavropoulos, M. Ležaić, B. Sanyal, G. Bihlmayer and S. Blügel
Appl. Phys. Lett. 103, 102404 (2013)

III **First principles calculation of exchange interactions, spin waves and temperature dependence of magnetisation in inverse-Heusler-based spin gapless semiconductors**
Adam Jakobsson, I. Galanakis, Ph. Mavropoulos, E. Şaşioğlu, M. Ležaić, B. Sanyal and S. Blügel
Manuscript

IV **Constraining fields, The Magnetic Force Theorem and Susceptibility Calculations**
A. Jakobsson, C. Etz, M. Ležaić, B. Sanyal and S. Blügel
Manuscript

The author also contributed to the following published scholarly work which is not included in this thesis:

i A. Edström, J. Chico, **A. Jakobsson**, A. Bergman, J. Rusz
Electronic structure and magnetic properties of $L1_0$ binary alloys
Physical Review B 90, 014402 (2014)
DOI: http://dx.doi.org/10.1103/PhysRevB.90.014402

Contents

1. Introduction

This thesis is a combination of method development, implementation and applications in the frozen magnon tradition. Motivated by the possibilities of significant technological development and the fun of doing science, the goal of the work presented here is to accurately describe magnetic material properties using the powerful tools available from density functional theory. The frozen magnon method was implemented in an all-electron full potential code in order to enable the accurate study of systems with any number of magnetic sub-lattices. The first main application considered in this thesis was the study

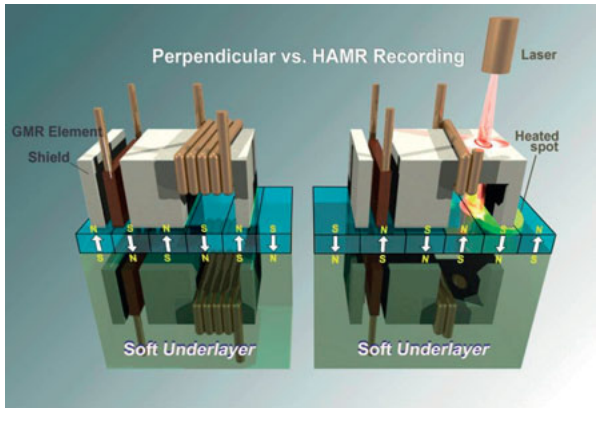

Figure 1.1. Perpendicular recording technique versus HAMR recording method. (Figure from Seagate & http://www.dailytech.com.)

of tetragonally distorted FeCo films as a candidate material for heat assisted magnetic recording (HAMR) storage media. The basic idea is that in order to increase the capacity of storage devices there is a need to find materials suitable for encoding spatially smaller and less volatile bits of information. The smaller and more compact the bits become (thus the higher the storage density) the more challenging it is to read and write to the material. One solution is to locally heat the storage media with a laser to make the bits less rigid for the manipulation by magnetic fields (see Fig. 7.1). This technology is not yet commercially available, but HAMR has enabled Seagate, a major commercial producer of storage media, to reach unprecedented capacity in prototypes and it encourages them to go even further towards the 1 TB on inch^2. We suggest tetragonally distorted FeCo as grown on a Rh substrate as a possible candidate

based on theoretical estimations of the critical temperature of the material and it's significant magnetic anisotropy.

In the second application, the focus is on the emerging field of spintronics for investigating a class of materials, namely the spin gapless semiconductors, where the conductivity of the material depends on the spin-polarisation of the charge carriers. Most of the materials in this study was only considered theoretically up-to-date and we provide additional information on magnetic properties in order to enable the experimentalists to do informed decisions on what materials to synthesise.

In the last part of this thesis, the impact of a central approximation used in the field, the magnetic force theorem, was addressed and the implemented frozen magnon method was adjusted to correct for the errors introduced by the approximation. Furthermore, an implementation of a different spin-spirals based method that entirely avoided this approximation was implemented with the expectation that it would give more consistently accurate results. Comparisons were made between the different methods and to date the newly implemented method that is based on the evaluation of the susceptibility seems to deliver improved results.

2. *Ab initio* Calculations

Since the rapid development of quantum theory at the beginning of the last century, it soon became apparent to physicists that while the theory was in principle in place to calculate material properties of solids, due to the complexity of the many body problem it was still impossible to do calculations from first principle without any approximations.

Motivated by the considerable larger mass of the ions relative to the electrons, the Born-Oppenheimer approximation might be assumed for solid state calculations in order to reduce their complexity. In this approximation the ions are considered as fixed points and hence the number of free-variables is greatly reduced. Within this approximation the many body Schrödinger equation for a system of N electrons and M ions takes the following form.

$$\left\{ -\sum_{i=1}^{N} \frac{\hbar^2}{2m} \nabla^2 + \sum_{i,j=1, i\neq j} \frac{e^2}{|\mathbf{r}_i - \mathbf{r}_j|} + \sum_{i=1}^{N} \sum_{\mu=1}^{M} \frac{e^2 Z^\mu}{|\mathbf{r}_i - \tau^\mu|} \right\} = E\Psi \tag{2.1}$$

Due to the Pauli principle the wave function has to be antisymmetric, which leads to solutions in the form of sums of Slater determinants. But even with the Born-Oppenheimer approximation further approximations have to be done in order to treat systems larger than a few electrons. With the development of density functional theory (DFT), a theoretical framework was provided for effective independent particles approaches that enabled the theoretical treatment of realistic solids.

2.1 Density Functional Theory

The central idea of DFT is to consider the electron density $\rho(\mathbf{r})$ instead of the full many-body wave functions $\Psi(\mathbf{r}_1, \ldots, \mathbf{r}_N)$ in order to reduce the number of free variables.

$$\rho(\mathbf{r}) = \left\langle \Psi | \sum_{i=1}^{N} \delta(\mathbf{r} - \mathbf{r}_i) | \Psi \right\rangle \tag{2.2}$$

This was motivated by two central theorems for systems with non-degenerate ground states proven by Hohenberg and Kohn[1] and later generalised by Levy.[2]

1. For any system of interacting particles in an external potential, the external potential is uniquely determined by the ground state density up to a constant shift. As a corollary, all properties of the system are determined by the ground state density since the Hamiltonian and the many body wave functions for all possible states of the system are determined.

2. There exist a universal functional for the energy in terms of the density $E(\rho)$ that is valid for any external potential and for any particular external potential the exact ground state energy of the system is the global minimum value of this functional. The density that minimises the energy functional is the ground state density. This implies that once $E(\rho)$ is known one can find the appropriate ground state density and energy for any external potential.

$$E[\rho] \geq E[\rho_0] \tag{2.3}$$

The theorems of Hohenberg and Kohn gave a justification to consider the electron density instead of the more complex many body wave functions but this provides little help in solving practical problems since the energy functional $E(\rho)$ is not known explicitly. However Kohn and Sham[3] provided an effective procedure to introduce approximate energy functionals.

They separated the energy functional into contributions coming from a fictitious system of non-interacting electrons with the same density as the system under consideration and gathered any further contributions into a term to be treated with suitable approximations.

$$E[\rho] = T_s[\rho] + U[\rho] + E_{xc}[\rho] \tag{2.4}$$

Here T_s is the kinetic energy of non-interacting electrons, $U(\rho)$ is the Coulomb energy formed by the Hartree energy and the external potential. i.e. the interactions between the electrons and the ions and any present external electromagnetic fields. The non-interacting systems is assumed to be described by a single Slater determinant of N single particle wave-functions $\psi_\nu(\mathbf{r})$ called Kohn-Sham orbitals. The electron density of the system is thus given by:

$$\rho(\mathbf{r}) = 2\sum_{\nu=1}^{N} |\psi_\nu(\mathbf{r})|^2 \tag{2.5}$$

This gives the following explicit expression for the kinetic energy and Coulomb energy disregarding any external electromagnetic field.

$$T_s[\rho] = -2\sum_{\nu=1}^{N} \int \psi_\nu^*(\mathbf{r}) \frac{\hbar^2}{2m} \nabla^2 \psi_\nu(\mathbf{r}) d^3r \tag{2.6}$$

$$U[\rho] = E_{ext}[\rho] + E_H[\rho] \tag{2.7}$$

$$E_{ext}[\rho] = -4\pi e^2 \sum_{\mu=1}^{M} \int \frac{\rho(\mathbf{r}) Z^{\mu}}{|\mathbf{r} - \tau^{\mu}|} d^3 r \tag{2.8}$$

$$E_H[\rho] = 4\pi \frac{e^2}{2} \int \frac{\rho(\mathbf{r})\rho(\mathbf{r}')}{|\mathbf{r} - \mathbf{r}'|} d^3 r d^3 r' \tag{2.9}$$

The exchange correlation energy $E_{xc}[\rho]$ is defined by subtracting the above expressions from the total energy functional Eq. (2.4). It contains contributions arising from corrections of the kinetic energy due to electron-electron interactions, exchange energy and further contributions of electron-electron interaction due the deviations from a single Slater determinant state, called correlation energy. In principle, also the exchange energy may treated exactly, but it has been shown that approximate expressions have worked well due to cancelation of errors for many applications [4]. Minimising the energy functional with respect to the Kohn-Sham orbitals leads to the Kohn-Sham equation.

$$\left\{ -\frac{\hbar^2}{2m} \nabla^2 + V_{eff} - \varepsilon_{\nu} \right\} \psi_{\nu}(\mathbf{r}) = 0 \tag{2.10}$$

All terms except the kinetic energy is collected in an effective potential V_{eff}.

$$V_{eff} = V_{ext} + V_H + V_{xc} \tag{2.11}$$

$$V_{ext} = -4\pi e^2 \sum_{\mu=1}^{M} \frac{Z^{\mu}}{|\mathbf{r} - \tau^{\mu}|} \tag{2.12}$$

$$V_H = 4\pi e^2 \int \frac{\rho(\mathbf{r}')}{|\mathbf{r} - \mathbf{r}'|} d^3 r \tag{2.13}$$

$$V_{xc} = \frac{\partial E_{xc}[\rho(\mathbf{r})]}{\partial \rho(\mathbf{r})} \tag{2.14}$$

Since the electron density appears in the effective potential an iterative process is needed to solve the Kohn-Sham equations. The Kohn-Sham orbitals provide a charge density which determines the effective potential which in turn updates the Kohn-Sham equations. This process is repeated until self-consistency is achieved. If the total energy of the electron-ion system is required, then the Madelung energy E_M accounting for the ion-ion interaction has to be added to the functional in Eq. (2.4).

2.2 Spin-Density Functional Theory

Density functional theory has to be extended beyond its basic concepts in order to enable the calculation of magnetic properties. Besides the electron density $\rho(\mathbf{r})$, the energy of the system is now considered to be a functional of the magnetisation density $\mathbf{m}(\mathbf{r})$ as well. The basic variational principle in Eq. (2.3) now becomes:

$$E[\rho(r),\mathbf{m}(r)] \geq E[\rho_0(r),\mathbf{m}_0(r)] \tag{2.15}$$

The Kohn-Sham wave functions are replaced with two component Pauli wave functions $\psi_{\alpha i}(\mathbf{r})$ capable of representing both the electron density and the magnetisation density. The α index here represents the spin states.

$$\rho(\mathbf{r}) = \sum_{\nu=1}^{N} \sum_{\alpha=1,2} |\psi_\nu(\mathbf{r})|^2 \tag{2.16}$$

$$\mathbf{m}(\mathbf{r}) = \sum_{\nu=1}^{N} \psi_\nu^*(\mathbf{r}) \sigma \psi_\nu(\mathbf{r}) \tag{2.17}$$

$$\sigma = \sigma_x \hat{\mathbf{x}} + \sigma_y \hat{\mathbf{y}} + \sigma_z \hat{\mathbf{z}} \tag{2.18}$$

Here σ_x, σ_y and σ_z are the Pauli matrices. From the variational principle one obtains the Kohn-Sham equations that are analogous to the Schrödinger-Pauli equations.

$$\left\{ -\frac{\hbar^2}{2m}\nabla^2 + V_{eff} + \sigma \cdot \mathbf{B}_{eff}(\mathbf{r}) - \varepsilon_\nu \right\} \psi_\nu(\mathbf{r}) = 0 \tag{2.19}$$

The effective magnetic field $\mathbf{B}_{eff}$ is composed by a contribution $\mathbf{B}_{xc}$ arising from the exchange correlation energy and a contribution $\mathbf{B}_{ext}$ from any external field.

$$\mathbf{B}_{eff} = \mathbf{B}_{xc} + \mathbf{B}_{ext} \tag{2.20}$$

$$\mathbf{B}_{xc} = \frac{\partial E_{xc}[\rho(\mathbf{r}),\mathbf{m}(\mathbf{r})]}{\partial \mathbf{m}(\mathbf{r})} \tag{2.21}$$

2.3 Energy Functionals

Even though the exact form of $E_{xc}[\rho(\mathbf{r}),\mathbf{m}(\mathbf{r})]$ in Eq. (2.4) is not known, various successful approximations have been applied. The most commonly used is the local spin density approximation [LSDA] where the exchange correlation energy at each point in space is the same as that of a homogenous gas with

the same charge- and magnetisation density. The exchange correlation energy then takes the following explicit form:

$$E_{xc}[\rho(\mathbf{r}),\mathbf{m}(\mathbf{r})] = \int \rho(\mathbf{r})\varepsilon_{xc}(n(\mathbf{r}),\mathbf{m}(\mathbf{r})) \tag{2.22}$$

where ε_{xc} is a parametrised function that may be obtained from Quantum Monte Carlo calculations[5] of a homogenous electron gas. The natural extension to the LDA functional is the generalised gradient approximation (GGA) functional [6]where ε_{xc} additionally takes into account the gradient of the charge density.

$$E_{xc}[\rho(\mathbf{r}),\mathbf{m}(\mathbf{r}),|\nabla\rho(\mathbf{r})|] = \int n(\mathbf{r})\varepsilon_{xc}(\rho(\mathbf{r}),\mathbf{m}(\mathbf{r}),|\nabla\rho(\mathbf{r})|) \tag{2.23}$$

Since the LSDA functional approximates the local exchange correlation potential with that of a homogenous electron gas it can be assumed that the approximation works well for smoothly varying electron densities. However, for systems with localised states the LSDA breaks down, failing to provide a proper description of material properties. For some systems, adding gradient corrections are not enough and procedures to deal with localised states has been suggested over the years such as the self-interaction corrections (SIC) scheme [7], LSDA+U [8, 9], dynamical mean field theory (DMFT) [10], hybrid functionals and self consistent GW calculations [11]. In the present work we considered the LSDA+U functional as implemented in Fleur [12]. The energy functional in the LSDA+U formalism is:

$$E[\rho(\mathbf{r}),\mathbf{m}(\mathbf{r}),\hat{n}] = E^{LDA}[\rho(\mathbf{r}),\mathbf{m}(\mathbf{r})] + E^{ee}[\hat{n}] - E^{dc}[\hat{n}] \tag{2.24}$$

Here $\hat{n}$ is an occupation matrix of a selected set of atomic orbitals localised at a specific ion site. In our case it is the 3-d orbitals of the transition metal ions. The term $E^{ee}[\hat{n}]$ is taken in accordance with the multi-band Hubbard model.

$$E^{ee}[\hat{n}] = \frac{1}{2}\sum_{m_1 m_2 m_3 m_4}^{\sigma,\sigma'} \hat{n}^{\sigma}_{m_1,m_2}\left((m_1,m_3|V^{ee}|m_2,m_4) - (m_1,m_3|V^{ee}|m_4,m_2)\delta_{\sigma,\sigma'}\right)\hat{n}^{\sigma'}_{m_1,m_2} \tag{2.25}$$

The term $E^{dc}[\hat{n}]$ in Eq. (2.24) is a double counting correction that is supposed to take care of the fact that the interactions among the d-electrons introduced by the electron-electron interaction term $E^{ee}[\hat{n}]$ is already treated in the LSDA functional. There are many different proposals on suitable double counting schemes, however the atomic limit double counting scheme is most widely used and is employed in this work. The double counting correction in the atomic limit is given by:

$$E^{dc}(\hat{n}) = \frac{U}{2}n(n-1) - \frac{J}{2}\sum_{\sigma} n^{\sigma}(n^{\sigma}-1) \tag{2.26}$$

were in this context n is the number of electrons in the states where the Hubbard U has been applied and n^{σ} gives the number of such electrons in the spin state σ. There are several ways in which to estimate the Hubbard U and Hund's J from *ab-initio* calculations such as constrained LSDA calculations [13], linear response theory and constrained random phase approximation [14], but in many cases U and J are determined through comparisons between some calculated property and experiments. Minimising Eq. (2.24) with respect to the Kohn-Sham orbitals leads to a modified Kohn-Sham equation.

$$\left\{ -\frac{\hbar^2}{2m}\nabla^2 + V_{eff} + \sigma \cdot \mathbf{B}_{eff}(\mathbf{r}) - \varepsilon_i \right\} \psi_i(\mathbf{r}) + \sum_{m,m'} V^{\sigma}_{mm'} \frac{\partial n^{\sigma}_{mm'}}{\partial \psi^{*\sigma}_{nu}} = 0 \tag{2.27}$$

The explicit form of $V^{\sigma}_{mm'}$ and $\dfrac{\partial n^{\sigma}_{mm'}}{\partial \psi^{*\sigma}_{nu}}$ may be found in the work of S. Shick et al.[12].

2.4 The Kohn-Sham Equations in a Periodic Potential

In a bulk solid neglecting defects and impurities we can assume a periodic potential, i.e. we have $V_{eff}(\mathbf{r}+\mathbf{R})$ where $\mathbf{R}$ is a Bravais lattice vector. Translational symmetry in the potential fulfils the condition of Bloch's theorem which proves that the Kohn-Sham orbital must also be periodic with respect to translations. [15]

$$\psi_{\nu,\mathbf{k}}(\mathbf{r}+\mathbf{R}) = e^{i\mathbf{k}\cdot\mathbf{R}}\psi_{\nu,\mathbf{k}}(\mathbf{r}) \tag{2.28}$$

The Kohn-Sham equations can be solved separately for each $\mathbf{k}$. So to obtain quantities such as the total number of electrons, the sum of eigenvalues or the charge density a summation has to be done over the $\mathbf{k}$-points in the irreducible Brillouin zone (IBZ). For an infinite solid the summation takes the form of an integral as follows:

$$\frac{1}{V_{IBZ}} \int_{IBZ} \sum_{\nu,\varepsilon_\nu<E_F} f_\nu(\mathbf{k}) d^3k \tag{2.29}$$

However, due to computational reasons we can only solve the Kohn-Sham equations for a finite number of $\mathbf{k}$-points, which implies that the integrals have to be discretized.

$$\frac{1}{V_{IBZ}} \int_{IBZ} \sum_{\nu,\varepsilon_\nu<E_F} f_\nu(\mathbf{k}) d^3k \longrightarrow \sum_{IBZ} \sum_{\nu,\varepsilon_\nu<E_F} f_\nu(\mathbf{k}) w(\mathbf{k}) \tag{2.30}$$

In the special point method this is done by assigning a weight $w(\mathbf{k})$ to every $\mathbf{k}$-point. The sum of the weights over all $\mathbf{k}$-points up to the Fermi energy gives the number of electrons per unit cell.

$$N = \sum_{IBZ} \sum_{\nu, \varepsilon_\nu < E_F} w(\mathbf{k}) \tag{2.31}$$

Hence by occupying the calculated bands starting from the lowest eigenvalues and summing the weights of the corresponding $\mathbf{k}$-points eventually the Fermi energy may be determined when the summation equals the number of electrons in a unit cell. However in order to avoid strong oscillations in the charge density and effective potential that can appear due to states being promoted or demoted across the Fermi surface, the Fermi energy is determined in each iteration by satisfying.

$$N = \sum_{IBZ} \sum_{\nu} w(\mathbf{k}) \frac{1}{e^{(\varepsilon_\nu(\mathbf{k}) - E_F)/k_B T} + 1} \tag{2.32}$$

Here k_B is the Boltzmann constant and T is a broadening temperature that can be adjusted to give a smooth convergence. This procedure is called Fermi smearing and has been used throughout this work. The temperature adjusted weights $w(\mathbf{k}, \varepsilon_\nu(\mathbf{k}) - E_F)$ may be stored and used for all Brillouin integrations.

$$w(\mathbf{k}, \varepsilon_\nu(\mathbf{k}) - E_F) = w(\mathbf{k}) \frac{1}{e^{(\varepsilon_\nu(\mathbf{k}) - E_F)/k_B T} + 1} \tag{2.33}$$

2.5 The Eigenvalue Problem

The Kohn-Sham equation is solved by expanding the one-electron wave function in a set of basis functions. Since we assume translational symmetry, such an expansion following Bloch's theorem has the form:

$$\psi_{\nu,\mathbf{k}}(\mathbf{r}) = \sum_{\mu} c_{\nu\mu\mathbf{k}} \varphi_{\mu,\mathbf{k}}(\mathbf{r}) \tag{2.34}$$

The Kohn-Sham equation (2.10) with an expansion such as (2.34), give rise to a generalised eigenvalue problem with Hamiltonian $H^{KS}_{\mu\mu'}(\mathbf{k})$ and overlap $S_{\mu\mu'}(\mathbf{k})$ elements.

$$\sum_{\mu'} [H^{KS}_{\mu\mu'}(\mathbf{k}) - \varepsilon_{\nu\mathbf{k}} S_{\mu\mu'}(\mathbf{k})] c_{\nu\mu'\mathbf{k}} = 0 \tag{2.35}$$

$$H^{KS}_{\mu\mu'}(\mathbf{k}) = \int_\Omega \varphi_{\mu\mathbf{k}}(\mathbf{r}) H^{KS} \varphi_{\mu'\mathbf{k}}(\mathbf{r}) d^3r \tag{2.36}$$

$$S_{\mu\mu'}(\mathbf{k}) = \int_\Omega \varphi_{\mu\mathbf{k}}(\mathbf{r}) \varphi_{\mu'\mathbf{k}}(\mathbf{r}) d^3r \tag{2.37}$$

A basis that is straightforward to implement is a set of plane waves since they automatically form an orthogonal set and are diagonal in any power of momentum making the calculation of the Hamiltonian elements simple. However, in order to describe the wave functions near the ions either a large basis set has to be used or pseudo-potentials must be employed [16]. Noticing that plane waves are solutions to a Hamiltonian with a constant potential while the solution of a spherically symmetric potential are products of spherical harmonics and radial functions, it seems natural to seek to improve the plane wave basis set by combining them with spherical harmonics for the description of the density near the ion cores.

2.6 The LAPW and APW+lo Methods

In the augmented plane wave method (APW) [17] the crystal cell is divided into two kinds of regions: spherical regions around the ions, called muffin-tins (MT), and an interstitial region (IR). Inside the muffin-tins the potential is set to be spherically symmetric while in the interstitial region the potential is usually set to a constant. This divisions of space makes it possible to define the augmented plane waves $\varphi_{\mathbf{G}}(\mathbf{k},\mathbf{r})$ that are combinations of plane wavess and atomic orbitals for the solution of the Kohn-Sham scheme.

$$\varphi_{\mathbf{G},\sigma}(\mathbf{k},\mathbf{r}) = \begin{cases} e^{i(\mathbf{G}+\mathbf{k})\cdot\mathbf{r}}\chi_\sigma \ \in IR \\ \\ \sum_{lm} A_{lm}^{\mu\mathbf{G}}(\mathbf{k}) u_l(r) Y_{lm}(\hat{\mathbf{r}})\chi_\sigma \ \in MT \end{cases} \tag{2.38}$$

Here $\mathbf{G}$ is a reciprocal lattice vector, $\mathbf{k}$ is a Bloch vector, l and m are the quantum numbers, $u_l(\mathbf{r})$ is the solution to the radial Schrödinger equations and χ_σ a Pauli spinor.

$$\left\{ -\frac{\hbar^2}{2m}\frac{\partial^2}{\partial r^2} + \frac{\hbar^2}{2m}\frac{l(l+1)}{r^2} + V(r) - E_l \right\} r u_l(r) = 0 \tag{2.39}$$

The coefficients $A_{lm}^{\mu G}(\mathbf{k})$ are found by the requirement of continuity at the border of the muffin-tin spheres. So the augmented plane wave basis functions are plane waves in the interstitial region and sums of the eigenfunctions that solve the radial Schrödinger equation for a spherical potential given a set of quantum numbers l and m and energy parameter E_l. With a fixed energy parameter one may obtain a regular eigenvalue problem through the Kohn-Sham scheme. However it has been shown that only by letting the energy parameters vary according to the calculated band energies accurate calculations can be done. [18] This leads to very computationally demanding calculations. The computational demands associated with the APW basis set made it fruitful to search for a way to circumvent the requirement that E_l has to be equal to the

calculated band energies. This is achieved in the linearized augmented plane wave method (LAPW)[19] where also the derivatives of the solutions of the radial Schrödinger equation are considered. This procedure make sense since the u_l functions can be expanded in a Taylor series around the energy parameter E_l. By keeping only the first two terms in the expansion, an error of the order $(\varepsilon - E_l)^2$ is introduced in the basis set and of the order $(\varepsilon - E_l)^4$ for the band energies. [18]

$$u_l(\varepsilon, r) = u_l(E_l, r) + \dot{u}_l(E_l, r) \tag{2.40}$$

The advantages of the linearized augmented plane waves are that the energy parameters can deviate from the band energies and total energies can be found by solving a simple secular problem. Even though the energy parameters are set to a constant value and the band energy naturally deviates from this value, accurate calculations can be performed due to the high order of the error. The explicit form of the basis functions is now the following.

$$\varphi_{\mathbf{G},\sigma}(\mathbf{k}, \mathbf{r}) = \begin{cases} e^{i(\mathbf{G}+\mathbf{k})\cdot\mathbf{r}}\chi_\sigma \ \in IR \\ \\ \sum_{lm}(A_{lm}^{\mu G}(\mathbf{k})u_l(r)Y_{lm}(\hat{\mathbf{r}}) + B_{lm}^{\mu G}(\mathbf{k})\dot{u}_l(r)Y_{lm}(\hat{\mathbf{r}}))\chi_\sigma \ \in MT \end{cases} \tag{2.41}$$

The APW and LAPW methods were originally formulated using a shape approximation on the electron potential. Inside the muffin tin the potential was considered to be spherically symmetric and outside often a constant potential was employed.

$$V(\mathbf{r}) = \begin{cases} V_I \ \in IR \\ \sum_{lm} V_{lm}^{\mu}(\mathbf{k})Y_{lm}(\hat{\mathbf{r}}) \ \in MT \end{cases} \tag{2.42}$$

This approximation is often reasonable in close packed systems but is less accurate for open structures. In the full potential augmented plane wave method (FLAPW)[20], no shape approximation is made and hence the potential of the following form is used.

$$V(\mathbf{r}) = \begin{cases} \sum_G V_I e^{i(\mathbf{G}\cdot\mathbf{r})} \ \in IR \\ \sum_{lm} V_{lm}^{\mu}(\mathbf{k})Y_{lm}(\hat{\mathbf{r}}) \ \in MT \end{cases} \tag{2.43}$$

Since the basis functions in the LAPW amethod are non-orthogonal we are left with a generalised eigenvalue problem to solve for each $\mathbf{k}$-point. This can however be reduced to a regular eigenvalue problem using a Cholesky decomposition [21].

More recently the APW+lo basis were suggested [22] as an alternative to the LAPW. Here the APW basis is complemented by local orbitals $\phi_{\sigma lm}$ that takes the value of zero in the interstitial region. This basis was shown to

increase the rate of convergence compared to a conventional LAPW basis. Both the Elk code and Fleur code have the possibility of using either basis set together with a potential without shape approximations.

$$\phi_{\sigma lm}(\mathbf{k},\mathbf{r}) = \begin{cases} 0 \in IR \\ \sum_{lm}(A^{\mu}_{lm}(\mathbf{k})u_l(r)Y_{lm}(\hat{\mathbf{r}}) + B^{\mu}_{lm}(\mathbf{k})\dot{u}_l(r)Y_{lm}(\hat{\mathbf{r}}))\chi_{\sigma} \in MT \end{cases} \tag{2.44}$$

2.7 Non-Collinear Magnetism

In this thesis we consider non-collinear magnetic structures and in particular different spin-spiral configurations. In the context of non-collinear magnetism it is useful to consider the density matrix ρ instead of the charge and magnetisation density. The density matrix is defined by:

$$\rho = \frac{1}{2}n\mathbf{I}_2 + \sigma\cdot\mathbf{m} = \begin{pmatrix} n+m_z & m_x - im_y \\ m_x + im_y & n-m_z \end{pmatrix} \tag{2.45}$$

In the same way the potential can be written in the compact form:

$$\mathbf{V} = V\mathbf{I}_2 + \mu_B\sigma\cdot\mathbf{B} = \begin{pmatrix} V+\mu_B B_z & \mu_B(B_x - iB_y) \\ \mu_B(B_x + iB_y) & V-\mu_B B_z \end{pmatrix} \tag{2.46}$$

The Kohn-Sham equation takes the following form:

$$\left\{-\frac{\hbar^2}{2m}\nabla^2\mathbf{I}_2 + \mathbf{V}\right\}\psi_{\nu} = \varepsilon_{\nu}\psi_{\nu} \tag{2.47}$$

Since the kinetic energy is diagonal with respect to the spin direction the only coupling terms between the spin up and spin down components of the Pauli spinor ψ_i are the terms $\mu_B(B_x - iB_y)$ and $\mu_B(B_x + iB_y)$. For a local potential such as the LSDA, it is always possible to find a local coordinate system that eliminates the x and y-components, which means that the usual collinear LSDA potential may be applied. This potential can later be rotated back to the global coordinate system providing the final non-collinear potential. This procedure is popularly called Kübler's trick, after being introduced by Jürgen Kübler [23].

In the Fleur implementation, magnetic collinearity within the muffin-tins is assumed and the magnetisation density changes direction only between the ionic sites. The impact of the approximation can therefore be varied and checked by a variation of the muffin-tin radius. For non-collinear structures outside the spin-spiral formalism, the collinearity is enforced through a constraining field $\mathbf{B}_c$ such that the perpendicular component of the magnetisation density becomes zero as integrated over the muffin-tin.

$$\int_{MT^\mu} \mathbf{m}(\mathbf{r}) d^3r - \hat{\mathbf{e}}^\mu \int_{MT^\mu} \hat{\mathbf{e}}^\mu \cdot \mathbf{m}(\mathbf{r}) d^3r = 0 \tag{2.48}$$

Here $\hat{\mathbf{e}}^\mu$ is the unit vector defining the local quantisation direction at the ion μ. However this procedure is not implemented for spin-spiral structures, which means that a small residual perpendicular component might be present in Fleur calculations. This is an issue that I believe will be corrected in the near future.

For the non-self consistent Fleur calculations, we rotate the muffin-tin potential in accordance with the chosen directions of the moments. This procedure results in a mismatch between the magnetisation in the muffin-tins and the magnetisation in the interstitial region which can be solved by setting the interstitial magnetisation density to zero.[24]

In the Elk code, we enforce the directions of the magnetic moments through the application of constraining fields that acts as Lagrange parameters in a constrained energy functional. The constraining fields are determined iteratively in the self-consistent calculations. The additional terms H_B in the Hamiltonian have the form:

$$H_B \sim \sigma \cdot \mathbf{B}^{\mathbf{c}} \tag{2.49}$$

2.8 Spin-Spirals and the Generalised Bloch Theorem

In a spin-spiral magnetic structure, the magnetic moments are rotated periodically in the crystal. The direction and periodicity of the rotation is described by a reciprocal lattice vector $\mathbf{q}$. Here we chose the global z-axis as the rotation axis, however this choice is arbitrary since we neglect spin orbit coupling. The magnetic moment $\mathbf{m}_{n\alpha}$ at an ion site $\mathbf{R}_{n\alpha}$ of the magnetic sub-lattice α and cell n can be written:

$$\mathbf{m}_{n\alpha} = m_\alpha(\sin(\theta)\cos(\mathbf{q}\cdot\mathbf{R}_{n\alpha}+\phi_\alpha), \sin(\theta)\sin(\mathbf{q}\cdot\mathbf{R}_{n\alpha}+\phi_\alpha), \cos(\theta)) \tag{2.50}$$

Here ϕ_α is a phase factor that depends on the sub-lattice α and θ is the cone-angle of the spin-spiral. The periodicity of the magnetic structure can be utilised to reduce the computational burden through the generalisation of Bloch's theorem [25, 26]. To prove this point it is useful to introduce the

translation operators $T_n = \{-\mathbf{q}\cdot\mathbf{R}_n|\varepsilon|\mathbf{R}_n\}$ that combine a regular translation by a lattice vector $\mathbf{R}_n$ with a rotation $\mathbf{U}(-\mathbf{q}\cdot\mathbf{R}_n)$ of the spinors around the z-axis with an angle $-\mathbf{q}\cdot\mathbf{R}_n$. Due to the periodicity of the magnetic structure we have:

$$H(\mathbf{r}+\mathbf{R}_n) = \mathbf{U}(\mathbf{q}\cdot\mathbf{R}_n)H(\mathbf{r})\mathbf{U}^{-1}(\mathbf{q}\cdot\mathbf{R}_n) \tag{2.51}$$

It is straightforward to show that the generalised translation operators form an abelian group of operators that commute with the Hamiltonian. The eigenstates of the Hamiltonian must therefore fulfil [15]:

$$T_n\psi(\mathbf{r},\mathbf{k}) = e^{i\mathbf{k}\cdot\mathbf{R}_n}\psi(\mathbf{r},\mathbf{k}) \tag{2.52}$$

This condition on the eigenstates can be shown to be equivalent to the statement that the eigenstates of the Hamiltonian must be of the form [27]:

$$\psi(\mathbf{r},\mathbf{k}) = e^{i\mathbf{k}\cdot\mathbf{r}}\begin{pmatrix} e^{-i\mathbf{q}\cdot\mathbf{r}/2}\,\alpha(\mathbf{r},\mathbf{k}) \\ e^{+i\mathbf{q}\cdot\mathbf{r}/2}\,\beta(\mathbf{r},\mathbf{k}) \end{pmatrix} \tag{2.53}$$

where $\alpha(\mathbf{r},\mathbf{k})$ and $\beta(\mathbf{r},\mathbf{k})$ are periodic functions. This results suggest that the spinor components should be multiplied by a term $e^{\mp i\mathbf{q}/2}$ where '$-$' sign holds for spin-up and '$+$' sign for spin down. The real beauty of the theorem becomes apparent when the the effective potential of the spin spiral system is applied on the modified basis. It can easily be shown that the Hamiltonian elements are similar to the non-collinear problem without the spiral, except for the contribution from the kinetic energy. This means that we can use the primitive crystallographic cell even for incommensurate spin spirals. To see this consider the Hamiltonian matrix elements generated by the potential $\tilde{\mathbf{V}}_{\mathbf{G},\sigma}$ for a spin-spiral state in the basis $\tilde{\varphi}_{\mathbf{G}}$.

$$\tilde{\varphi}_{\mathbf{G},\sigma}(\mathbf{k},\mathbf{r}) = \mathbf{U}(\mathbf{q}\cdot\mathbf{R}_n)\varphi_{\mathbf{G},\sigma}(\mathbf{k},\mathbf{r}) \tag{2.54}$$

$$\tilde{\mathbf{V}}_{\mathbf{G},\sigma}(\mathbf{k},\mathbf{r}) = \mathbf{U}(\mathbf{q}\cdot\mathbf{R}_n)\mathbf{V}_{\mathbf{G},\sigma}(\mathbf{k},\mathbf{r})\mathbf{U}^{-1}(\mathbf{q}\cdot\mathbf{R}_n) \tag{2.55}$$

$$\int_\Omega \tilde{\varphi}^*_{\mathbf{G},\sigma}(\mathbf{k},\mathbf{r})\tilde{\mathbf{V}}_{\mathbf{G},\sigma}(\mathbf{k},\mathbf{r})\tilde{\varphi}_{\mathbf{G},\sigma}(\mathbf{k},\mathbf{r})d\mathbf{r} = \int_\Omega \varphi^*_{\mathbf{G},\sigma}(\mathbf{k},\mathbf{r})\mathbf{V}_{\mathbf{G},\sigma}(\mathbf{k},\mathbf{r})\varphi_{\mathbf{G},\sigma}(\mathbf{k},\mathbf{r})d\mathbf{r} \tag{2.56}$$

3. Heisenberg Model Calculations

In the previous section a description was made of the ab-initio method we use in order to obtain the total energies of spin-spiral configurations. In this section it is shown how the total energy differences of spin-spiral configurations can be used to obtain exchange parameters for the classical Heisenberg model. Furthermore we generalise the well known one lattice equation that directly relate difference in spin-spiral total energies to adiabatic magnon dispersion to general multi-magnetic-lattice system.

The use of the magnetic force theorem (MFT) to get non-self consistent total energy differences is discussed. Even though several well developed procedures exists for correcting the MFT is seems that consistent improvements are difficult to obtain. For this reason we implemented a spin spiral based calculation procedure to obtain exchange parameters directly from the **q**-dependence of constraining fields. Furthermore it is shown that conceptually this method is similar to the method developed by Grotheer et. al. [28, 29]

Common to both methods is the application of the adiabatic approximation. In this approximation it is assumed that for the system under consideration the fast spin degrees of freedom from single-electron spin fluctuations are neglected and only the dynamics of the atomic moments on a time scale defined by the inverse frequencies of typical long-wavelength magnons are relevant [30].

3.1 Exchange Parameters from Total Energy Calculations

Our point of departure is a classical Heisenberg model, where normalised direction vectors of the magnetic moments $\mathbf{e}_{\mathbf{m}\alpha}$ are localised at ionic sites $\mathbf{R}_{\mathbf{m}\alpha}$ defined by a lattice vector $\mathbf{R}_{\mathbf{m}}$ and position vector τ_α of the magnetic Bravais lattice within a unit cell.

$$\mathbf{R}_{\mathbf{m}\alpha} = \mathbf{R}_{\mathbf{m}} + \tau_\alpha \tag{3.1}$$

The Heisenberg Hamiltonian H is the sum over all exchange parameters $J_{mn}^{\alpha\beta}$.

$$H = -\frac{1}{2N} \sum_{mn\alpha\beta} J_{mn}^{\alpha\beta} \mathbf{e}_{\mathbf{m}\alpha} \cdot \mathbf{e}_{\mathbf{n}\beta} \tag{3.2}$$

N is the number of unit cells in the crystal and the direction vectors $\mathbf{e}_{m\alpha}$ are given by:

$$\mathbf{e}_{m\alpha} = \sin\theta\cos(\mathbf{q}\cdot\mathbf{R}_{m\alpha})\mathbf{x} + \sin\theta\sin(\mathbf{q}\cdot\mathbf{R}_{m\alpha})\mathbf{y} + \cos(\theta)\mathbf{z} \tag{3.3}$$

The Heisenberg model is only valid locally for each particular magnetic configuration. In order to extract meaningful exchange parameters we are therefore restricted to small perturbations of the reference state, typically the ground state. [31]. It is thus necessary to only consider a small cone angle θ. The exchange parameters may be obtained from the following spin spiral total energy differences for each wave vector $\mathbf{q}$:

$$\begin{aligned} &\frac{2}{\sin^2\theta}(E_{\alpha\alpha}[\mathbf{0},\theta] - E_{\alpha\alpha}[\mathbf{q},\theta]) \\ &= \sum_n J_{0n}^{\alpha\alpha}\ (1-\cos(\mathbf{q}\cdot\mathbf{R}_{n\alpha})) \end{aligned} \tag{3.4}$$

$$\begin{aligned} &\frac{2}{\sin^2\theta}(E_{\alpha\beta}[\mathbf{0},(\theta)] - E_{\alpha\beta}[\mathbf{q},(\theta)]) \\ &= 2\sum_n J_{0n}^{\alpha\beta}\ (1-\cos(\mathbf{q}\cdot(\mathbf{R}_{0\alpha}-\mathbf{R}_{n\beta}))) \\ &+ \sum_n J_{0n}^{\alpha\alpha}(1-\cos(\mathbf{q}\cdot\mathbf{R}_{n\alpha})) \\ &+ \sum_n J_{0n}^{\beta\beta}(1-\cos(\mathbf{q}\cdot\mathbf{R}_{n\beta})) \end{aligned} \tag{3.5}$$

In this formalism $E_{\alpha\beta}[\mathbf{q},\theta]$ denotes the energy of a spin spiral with a wave vector $\mathbf{q}$, where a non-zero cone angle has been assigned only to the sub lattices α and β. A least square fitting procedure is applied to solve the system of equations. Further details on the method are supplied in paper I.

3.2 Magnons and Spin-Spiral Total Energies

The exchange parameters can related to magnon frequencies $\omega_{\mathbf{q}}$ through the framework of classical spin dynamics. [32] We obtain $\omega_{\mathbf{q}}$ for collinear spin-configurations as the eigenvalues of the spin-wave dynamical matrix.

$$\Delta_{\alpha\beta}(\mathbf{q}) = 2\left(\delta_{\alpha\beta}\sum_\gamma \frac{J^{\alpha\gamma}(\mathbf{0})M_\gamma}{|M_\alpha||M_\gamma|} - \frac{J^{\alpha\beta}(\mathbf{q})M_\beta}{|M_\alpha||M_\beta|}\right) \tag{3.6}$$

$$J^{\alpha\beta}(\mathbf{q}) = \sum_n J_{0n}^{\alpha\beta}\cos(\mathbf{q}\cdot(\mathbf{R}_{0\alpha}-\mathbf{R}_{n\beta})) \tag{3.7}$$

In the case of one magnetic sub-lattice, i.e. a simple ferromagnet this expression reduces to the following familiar form with quadratic dispersion close to the Γ-point.

$$\omega_{\mathbf{q}} = 2\frac{J(\mathbf{0}) - J(\mathbf{q})}{M} \tag{3.8}$$

Since the Fourier transformed exchange constants are directly related to spin-spiral total energies [24] it is possible to calculate magnon energies without explicit calculations of the real space exchange parameters. The spin-wave dynamical matrix is formed with matrix elements given directly from energy differences of spin-spiral total energies may be derived from (3.6) and the expression for the total energy of spin-spirals as given in paper I. The diagonal and off-diagonal elements are respectively given by the following equations:

$$\begin{aligned}\Delta_{\alpha\alpha}(\mathbf{q}) &= \frac{2}{|M_\alpha|\sin^2\theta}\times \\ &\left(\frac{2M_\alpha}{|M_\alpha|}(E^0_{\alpha\alpha}(\mathbf{q}) - E^0_{\alpha\alpha}(\mathbf{0})) + \sum_{\gamma\neq\alpha}\frac{M_\gamma}{|M_\gamma|}(E^{\pi/2}_{\alpha\gamma}(\mathbf{0}) - E^0_{\alpha\gamma}(\mathbf{0}))\right)\end{aligned} \tag{3.9}$$

$$\begin{aligned}\Delta_{\alpha\beta}(\mathbf{q}) &= \frac{2}{|M_\alpha|\sin^2\theta}\times \\ &\left(\frac{M_\beta}{|M_\beta|}(E^0_{\alpha\beta}(\mathbf{q}) - E^{\pi/2}_{\alpha\beta}(\mathbf{0})) - \sum_{\gamma=\alpha,\beta}\frac{M_\gamma}{|M_\gamma|}(E^0_{\gamma\gamma}(\mathbf{q}) - E^0_{\gamma\gamma}(\mathbf{0}))\right)\end{aligned} \tag{3.10}$$

In the case of one magnetic sub-lattice equation Eq. (3.9) reduces to the following well known expression.

$$\omega_{\mathbf{q}} = 4\frac{E(\mathbf{q},\theta) - E(\mathbf{0},\theta)}{M\sin^2\theta} \tag{3.11}$$

We note that our expressions in Eq. (3.9) and (3.10) deviate from those in a recent publication [33]. However it is clear that an unfortunate mathematical error has been introduced in the derivation of the magnon energies in that publication. It is not considered that the magnon energies in Eq. (27) in Ref. [33] are functions of $Re[\bar{J}^{\mathbf{q}}_{12}]^2$ and a change of sign upon translation by a reciprocal lattice vector $Re[\bar{J}^{\mathbf{q}}_{12}] \rightarrow -Re[\bar{J}^{\mathbf{q}+\mathbf{b}}_{12}]$ is thus irrelevant for the periodicity of the magnon energies, i.e. we still have $\omega_{\mathbf{q}} = \omega_{\mathbf{q}+\mathbf{b}}$. Hence their conclusion that the off-diagonal matrix elements in the spin-dynamical matrix should be zero is incorrect.

Eqs. (3.9) and (3.10) are equivalent to Eq. (3.8) and thus capture the known features of magnon dispersion curves such as the linear dispersion relation near the Γ-point and relatively small deviations from the second nearest neighbour approximation for the anti-ferromagnetic transition metal monoxides. The latter is expected since we can show that long-range exchange parameters are relatively small. None of these characteristics of antiferromagnetic transition metal monoxides appear in the calculated dispersion curves of Ref. [33].

3.3 The Magnetic Force Theorem

Since the size of the basis of non-collinear magnetic calculations is doubled compared to collinear calculations, the computational cost of spiral calculations scale quickly with an increased cut-off in the plane wave or angular momentum for the LAPW or APW+lo basis. For this reason, small accurate energy differences between spin spiral structures, which is the cornerstone of this thesis, are very computationally costly to obtain. For this reason it has long been a standard practice in the field to turn to the magnetic force theorem (MFT) [34], which states that the total energy difference of neighbouring magnetic states can be approximated by the difference in sums of single particle eigenvalues as obtained from the Kohn-Sham equations.

$$E(\mathbf{q}) - E(\mathbf{0}) = \sum_{occ} \varepsilon_\nu(\mathbf{q}) - \sum_{occ} \varepsilon_\nu(\mathbf{0}) + \mathscr{O}_2(\delta\rho, \delta\mathbf{m}) \tag{3.12}$$

Since the MFT is central to obtaining total energy differences between non-collinear states for a moderate cost in many methods of extracting exchange parameters, an extensive discussion can be found on the validity of the approximation.

V. Antropov [35], P.Bruno [36] and Katsnelson et al. [37] showed in separate works within the framework of multiple scattering theory, that the "bare" exchange parameters should be corrected in order to correspond to exchange parameters as derived from inverse dynamic magnetic susceptibility. P. Bruno [36] in particular recognised that the constraining fields that fixed the direction of the magnetic moments were neglected in major applications of the MFT, while they in principle should affect the eigenvalue sums, and suggested an appropriate renormalisation of the exchange parameters. Their methods were applied on bcc Fe and fcc Ni and it was found that the corrected exchange parameters yielded increasing magnon excitation energies and critical temperatures for both systems compared to results obtained with the exchange parameters using the "bare" MFT. This was not an unproblematic result since increasing magnon excitation energies for bcc Fe worsened the agreement with experimental results.

Katsnelson et al. [37] suggested that the success of the "bare" MFT in the case of bcc Fe is due to error cancelation and that reason the "bare" exchange parameters should still be applied for magnon excitations, while the critical temperature should be evaluated with renormalised exchange parameters. However, since the error cancelation is specific to bcc iron it seems that the procedure should not be generalised. Indeed, we show in paper IV that for B2 structured FeCo the "bare" MFT introduce large errors in the dispersion of spin-spirals that can successfully be corrected only with a procedure analogous to P. Bruno's renormalisation.

In non-self consistent spin spiral total energy calculations the Γ - point potential is used for all spin spirals regardless of their wave vector $\mathbf{q}$ and Eq. (3.12) is applied to obtain the total energy differences. In our procedure, that in the framework of the frozen magnon approach is the analogue of P. Bruno's renormalisation, we apply pre-converged constraining fields on each site. These fields have been converged pseudo-self consistently (in a previous step) with a frozen Γ - point potential. The same qualitative changes in the calculated exchange parameters, the magnon dispersion and critical temperature for bcc Fe is found as for the previously mentioned approaches.

Examples of methods that do not rely on the "bare" MFT are calculations of the full dynamical magnetic susceptibility [38] or its static limit. We have implemented a version of the inverse static transverse susceptibility (ISTS) method developed by Grotheer et al. [28, 29] since it avoids the complications introduced by the MFT. The implementation is described in the next section and we compare our results with the MFT based frozen magnon results in paper IV.

It is interesting to note that in non-collinear systems, the relative directions of the magnetic moments are a result of the competition between electronic exchange and kinetic energy. [28] In the framework of the generalised Bloch theorem and non-self consistent spin-spiral calculations it becomes very obvious, since we literarily only change the kinetic energy contribution to the Hamiltonian between different spin spiral structures (for a given set of cone angles).

3.4 Exchange Parameters from Susceptibility Calculations

Assuming a Heisenberg Hamiltonian we immediately obtain a relation between the exchange parameters and the ratio of an applied external magnetic field to the resulting magnetic moments, i.e. the static magnetic susceptibility.

$$\sum_{\mathbf{R}'} \mathbf{m}_{\mathbf{R}'} \cdot \mathbf{B}^{\mathbf{t}}_{\mathbf{R}'} = \sum_{\mathbf{R}'} \mathbf{m}_{\mathbf{R}'} \cdot \mathbf{B}^{\mathbf{c}}_{\mathbf{R}'} - \frac{1}{2} \sum_{\mathbf{R}\mathbf{R}'} J_{\mathbf{R}\mathbf{R}'} \mathbf{e}_{\mathbf{R}} \cdot \mathbf{e}_{\mathbf{R}'} \tag{3.13}$$

The derivative of the total energy expression (Eq. (3.13)) with respect to the direction vector $\mathbf{e}_{\mathbf{R}'}$ of the magnetic moment at site $\mathbf{R}'$, yields the following field equation:

$$m_{\mathbf{R}'}\mathbf{B}^{\mathbf{t}}_{\mathbf{R}'} = m_{\mathbf{R}'}\mathbf{B}^{\mathbf{c}}_{\mathbf{R}'} - \sum_{\mathbf{R}} J_{\mathbf{R}\mathbf{R}'}\mathbf{e}_{\mathbf{R}} \tag{3.14}$$

The $\mathbf{q}$-dependence comes from the form of the direction vector $\mathbf{e}_{\mathbf{R}}$.

$$\mathbf{e}_{\mathbf{R}} = \sin\theta\cos(\mathbf{q}\cdot\mathbf{R})\mathbf{x} + \sin\theta\sin(\mathbf{q}\cdot\mathbf{R})\mathbf{y} + \cos(\theta)\mathbf{z} \tag{3.15}$$

This enables us to define the inverse static transverse magnetic susceptibility $\chi^{-1}_{\mathbf{R}\mathbf{R}'}$ by:

$$\chi^{-1}_{\mathbf{R}\mathbf{R}'} = \delta_{\mathbf{R}\mathbf{R}'}\frac{B^{t,x}_{\mathbf{R}'}}{m^{x}_{\mathbf{R}'}} + (1-\delta_{\mathbf{R}\mathbf{R}'})\frac{J_{\mathbf{R}\mathbf{R}'}}{m^{x}_{\mathbf{R}}m^{x}_{\mathbf{R}'}} \tag{3.16}$$

Finally the relations between the applied constraining fields and the inverse susceptibility is given by:

$$\sum_{\mathbf{R}} \chi^{-1}_{\mathbf{R}\mathbf{R}'} m^{x}_{\mathbf{R}} = B^{c,x}_{\mathbf{R}'} \tag{3.17}$$

Equations (3.16) and (3.17) relate our approach to previous studies done along the same line by Grotheer et al. [29, 28] The main difference with respect to our approach is that they explicitly calculated the static susceptibility in reciprocal space, which they then invert in order to get the magnon dispersion. In our approach we consider the x-component of the field equation, Eq. (3.14), to calculate directly the exchange parameters in real space using a least squares fitting (LSF) procedure, similar to the one we implemented in paper I. A further difference is they apply a fixed external field and evaluate the resulting directional vectors $\mathbf{e}_{\mathbf{R}}$, while we evaluate the constraining fields necessary for fixed directional vectors.

A major advantage of this method is that for each considered spin-spiral calculation we obtain N sets of constraining fields and N resulting moments, where N is the number of magnetic sub lattices in the system. That means that we obtain the necessary values N rows in our system of equations. On the other hand in the conventional frozen magnon technique we only obtain a single value - the total energy for each calculation. This makes the scaling of the ISTS method favourable over the conventional frozen magnon technique. Furthermore the constraining fields converge much faster with respect to the number of $\mathbf{k}$-points compared to the fine energy differences in conventional frozen magnon calculations. Together these considerations imply a significant reduction in computational cost compared to self consistent spin spiral calculations making the method comparable to non-self consistent frozen magnon calculations.

4. Key Results

4.1 Test case bcc Fe

After implementing the frozen magnon method in the Fleur code according to the procedure detailed in paper I, we made numerous tests to investigate how the construction of the sets of spin-spirals affect the numerical stability of the least squares problem. One alternative we considered was to calculate spin spirals for **q**-points selected along paths that follow high-symmetry lines in the Brillouin zone. The motivation behind this choice was to employ the crystal symmetries that were compatible with the spin-spiral wave vectors in the *ab-initio* calculations and thus reduce the computational costs.

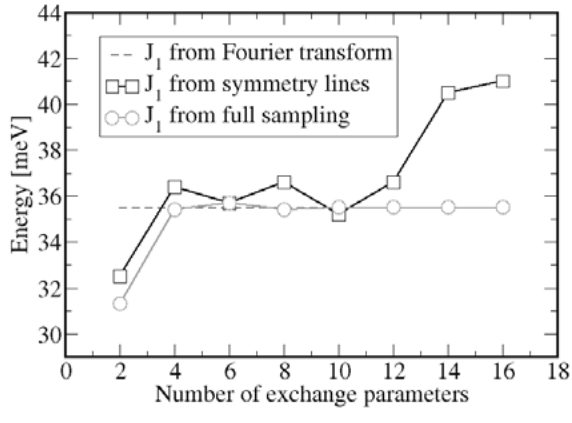

Figure 4.1. The convergence of the nearest neighbor exchange parameter in bcc Fe as a function of the number of exchange parameters used in the least squares fitting. Figure from Paper I: [32], copyright (2013) by APS.

As an example, we present the case of bcc Fe in Fig. 4.1. It is clear that this restriction of spin-spirals to the high-symmetry lines (Γ-N-P-Γ-H-N) led to poor numerical stability as compared to the "full sampling" procedure, where we scattered wave-vectors randomly in the first Brillouin zone. The latter approach was employed henceforth for all the calculations presented in this thesis. In Fig. 4.1 it is also shown that the results of the previously implemented, Fourier based, method of extracting exchange parameters corresponds exactly

to the results of the least squares approach if sufficiently many exchange parameters are taken into account.

A possible approach could be to combine a number of high symmetry points with an increasing number of general points depending upon the number of required exchange interactions. This would provide a numerically stable least squares fitting procedure, while some reduction in the computational costs could be achieved, especially for high symmetry crystals with a few dominating short range interactions.

4.2 Transition-Metal Monoxides

The transition metal monoxides NiO and MnO adopt the rocksalt structure in the paramagnetic phase. Below the Nèel temperature, an antiferromagnetic ordering sets in, where the direction of the atomic moments alternates between neighboring [111] planes (Fig. 4.2). The anti-ferromagnetic ordering is a result of strong superexchange interaction between each transition metal ion and its next nearest neighbors. Exchange-striction leads to a simultaneous magnetic and structural phase transition where the rocksalt structure is distorted into a trigonal structure.

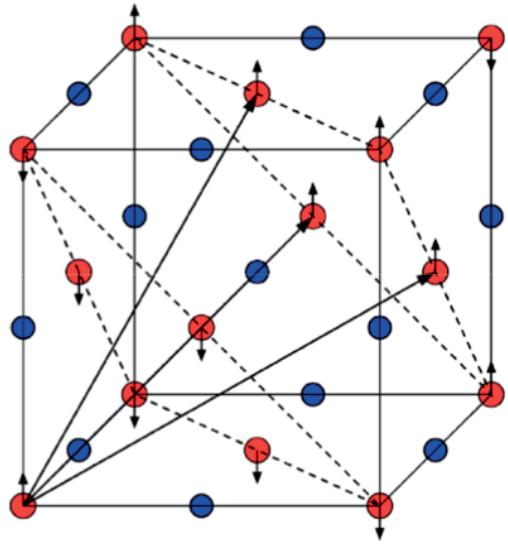

Figure 4.2. The chemical and magnetic structure of the transition metal monoxides NiO and MnO with their alternating spin-planes in the [111] direction. The lattice vectors of the magnetic unit cell are depicted by bold arrows.

MnO and NiO are known for having strong correlation effects associated with the 3*d*-electrons localized on the transition-metal ions. DFT functionals such as the local spin density approximation (LSDA) and the generalized gradient approximation (GGA) are not able to describe strong electron correlation. Beyond DFT methods such as the LSDA+U [39, 40, 41, 42, 43], Self interaction corrected (SIC) [44, 45, 46], dynamical mean field theory (DMFT) [47] and hybrid funtionals [48, 49, 50] have been employed with greater success improving the correspondence between calculated and experimental properties such as lattice parameters, band gaps and excitation energies for magnons and phonons.

To my knowledge, previous to this study, no full potential LSDA+U results have been published using an accurate method for obtaining exchange parameters (I don't consider the evaluation of exchange parameters by total energy differences of different collinear states as an accurate method). Furthermore, the results for MnO, employing the atomic sphere approximation (ASA) for the potential, indicated that the LSDA+U was inappropriate for the description of the magnetic properties of the system. The calculated ratio between the nearest and second nearest neighbour interaction differed significantly from the experimentallv obtained ratio.

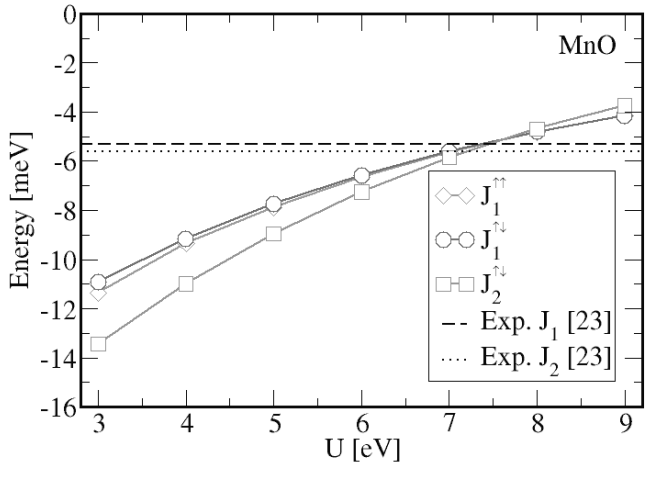

Figure 4.3. Exchange parameters in MnO (nearest and next-nearest neighbours) obtained for different values of Hubbard U. The available experimental values (Exp. [23], refers to Dudarev et al. [Phys. Rev. B 57, 1505]) are given with dotted lines for nearest neighbour and dashed lines for next nearest neighbour exchange parameters. Figure from Paper I: [32], copyright (2013) by APS.

In Fig. 4.3 the results for the nearest and second nearest neighbour exchange parameters are shown for values of Hubbard U from 3 to 9 eV. For MnO it is seen that U $\simeq$ 7 eV reproduces the experimental situation with the LSDA+U functional.

Solovyev et al. [40] showed that the experimental magnon dispersion could be obtained by adjusting the exchange splitting and charge transfer energy, the first being the difference in energy between majority and minority d-band and the second the difference in energy between the oxygen $2p$-states and the minority d-band. These quantities are crucial in determining the strength of the various exchange mechanisms in magnetic oxides.

For instance the direct exchange, that is relevant to nearest neighbour interactions depends on the exchange splitting, while the 180° super-exchange is the dominant contributor to the next nearest neighbour interaction and depends both on the exchange splitting and the charge transfer energy. This discussion implies that the full potential treatment gives a significantly more accurate exchange splitting and charge transfer energy than the ASA.

The trigonal distortion raises the degeneracy of $J_1^{\uparrow\uparrow}$ and $J_1^{\uparrow\downarrow}$, since the distance to the neighbours within the [111] plane will be larger than the neighbours outside the [111] plane. This implies that the direct overlap of the d-states of neighbouring atoms becomes different, thus affecting the direct exchange contribution, while changes in angles may affect the 90° super-exchange contribution. A volume conserving tensor T with a distortion parameter δ may be applied to make the transition between the cubic and trigonal structures.

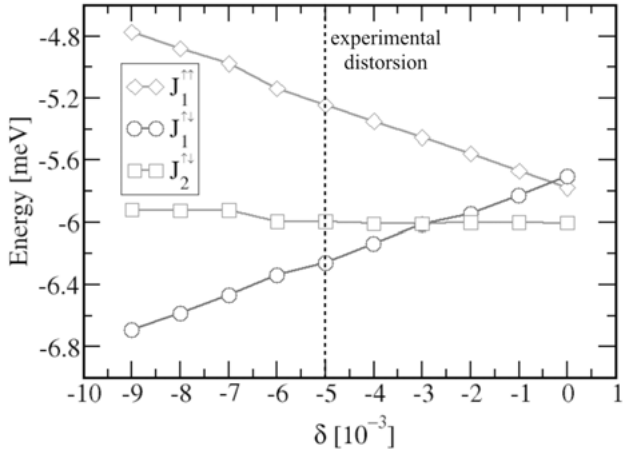

Figure 4.4. Nearest neighbour exchange parameters in MnO, as a function of the trigonal distortion δ. The experimental value of the distortion is marked by the vertical dashed line. These values were obtained for U = 6.9 eV and J = 0.86 eV. Figure from Paper I: [32], copyright (2013) by APS.

$$T = \frac{1}{(1+3\delta)^{1/3}} \begin{pmatrix} (1+\delta) & \delta & \delta \\ \delta & (1+\delta) & \delta \\ \delta & \delta & (1+\delta) \end{pmatrix} \tag{4.1}$$

Indeed it has been assumed that changes in the nearest neighbor exchange parameters are the main reasons for the exchange-striction effect in the transition-metal monoxides [45] and a calculation of the exchange parameters of MnO gives a significant dependence upon the distortion parameter as seen in Fig. 4.4.

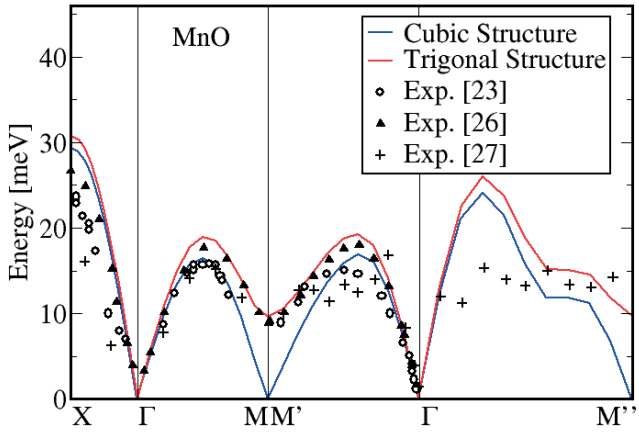

Figure 4.5. Comparison between experimental and calculated magnon dispersion curve for MnO. Exp. [23] refers to the work of G. Pepy [J. Phys. Chem. Solids 35, 433], Exp. [26] shows results of M. Kohgi et al. [J. Phys. Soc. Jpn. 36, 112] while Exp. [27] are data from A.L. Goodwin et al. [Phys. Rev. B 75, 075423]. For calculations we consider both the ideal rocksalt structure (blue line) and a trigonal structure (red line) defined by a distortion parameter $\delta = -0.005$. (U = 6.9 eV and J = 0.86 eV). Figure from Paper I: [32], copyright (2013) by APS.

In Fig. 4.5, the magnon dispersion curve for MnO in the cubic structure is shown in addition to the curve for the experimental trigonal structure. All exchange parameters that are of the order of 0.1 meV or larger are included. An excellent agreement with the experimental results is obtained when the experimental structure is assumed for MnO. It is shown that the non-zero energy obtained experimentally [51, 52, 53] at the M/M'-point in MnO is due to the trigonal distortion introduced by exchange striction.

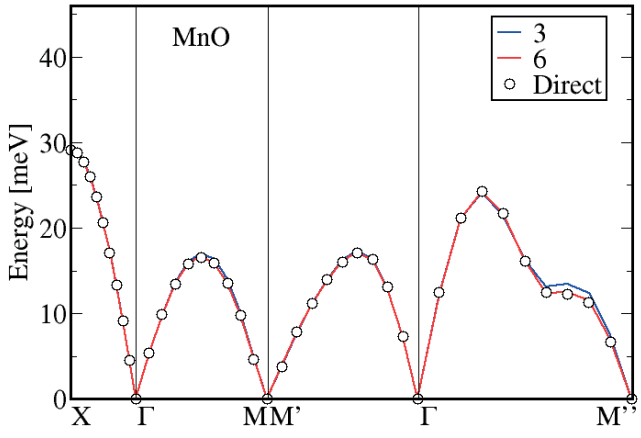

Figure 4.6. Magnon dispersion for MnO in the cubic structure for 3 and 6 exchange parameters, using Eq. (3.6). The "Direct" curve is calculated with Eq. (3.9) and (3.10) and represents the infinite limit. (with U = 6.9 eV and J = 0.86 eV) Figure from Paper I: [32], copyright (2013) by APS.

In Fig. 4.6 the magnon energies are shown for 3 and 6 included exchange parameters and compare these with the curves produced by using Eq. (3.9) and (3.10) that represent the infinite limit. Minor changes can be seen when increasing the number of exchange parameters from 3 to 6. We can see that further increases will not introduce noticeable changes in the dispersion curves since the curves produced with 6 parameters and curves given by the infinite limit are on top of each other.

4.3 Magnetic Properties of Distorted B2 structured FeCo

Motivated by previous works on tetragonally distorted B2 structured FeCo that suggested the material as a possible candidate for HAMR applications [38], the dependence of the Curie temperature (T_C) of the distortion was investigated. Experimentally the tetragonal distortion may be tuned by growing a film of FeCo on a substrate with an appropriate lattice structure. If the structural mismatch between the film and the substrate is small, then it might be energetically favourable for the film to adjust its structure to the substrate. FeCo has been successfully grown on Pd, Ir and Rh substrates [54], giving a tetragonal structure with progressively higher c/a ratio.

The frozen magnon method was applied as implemented in the Fleur code according to the procedure detailed in paper I. In the light of the later results of paper IV the quantitative results, as reported in paper II, should be checked with a method that doesn't rely on the MFT. However, the main qualitative conclusions may still apply and a short summary is given here.

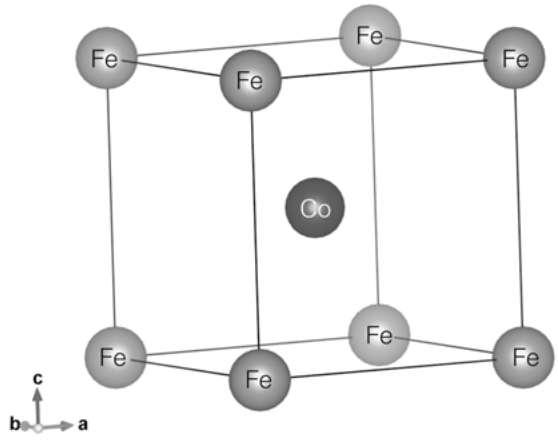

Figure 4.7. The structure of B2 FeCo. Created with VESTA [55].

For the B2-type FeCo compound the tetragonal distortion reduces the T_C. The T_C decreases monotonically from 1575 K (for c/a = 1) to 940 K (for c/a = $\sqrt{2}$). The changes of the nearest neighbor Fe-Co exchange interaction are sufficient to explain the c/a behaviour of the T_C, as can be seen from Fig. 4.8. The first reason is that the value is significantly larger than the value of the Co-Co or Fe-Fe parameters. Secondly, they closely follow the monotonical reduction of T_C with increasing distortion, except for a flattening-out of T_C close to c/a = $\sqrt{2}$.

And thirdly, even though the intra-sublattice exchange interactions show strong variations with tetragonal distortion compared to the Fe-Co interaction, these interactions differ in sign and thus largely cancel out in their contribution to the T_C. Only close to the end of the interval at c/a = $\sqrt{2}$ do the Co-Co and Fe-Fe interactions contribute significantly towards a stronger ferromagnetic coupling, which results in a flattening-off of the curve of T_C close to c/a = $\sqrt{2}$.

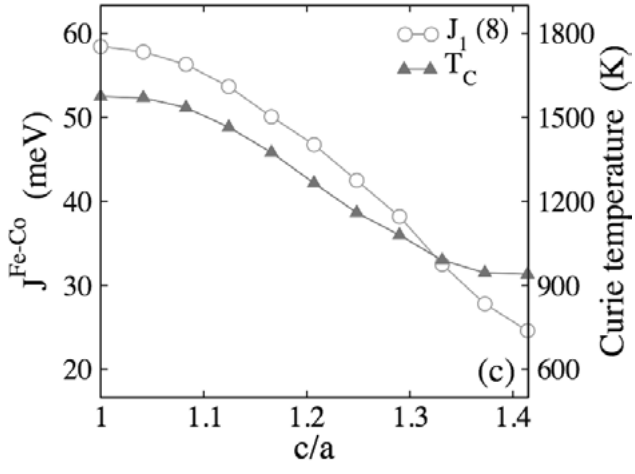

Figure 4.8. Inter-sublattice Fe-Co exchange interactions and critical temperature variation (blue curve) as a function of changes in the c/a ratio.

The behaviour of the exchange interactions with the changes in the c/a ratio and the resulting reduction of T_C can be attributed to different exchange mechanisms that are discussed qualitatively in paper II. The moderate T_C value suggests that FeCo grown on the Rh substrate with c/a = 1.24 could be a promising material for HAMR applications.

4.4 Magnetic Properties of Inverse Heusler Materials

In half-metallic magnets there is a metallic majority-spin electronic band structure and a semiconducting minority-spin electronic band structure.[56, 57] Such compounds could lead to the creation of a fully spin-polarised current, maximising the efficiency of spintronic devices. A class of materials bridging the gap between half-metals and magnetic semiconductors are the so-called spin-gapless semiconductors (SGS); where there is an almost vanishing zero-width energy gap at the Fermi level in the majority-spin direction and a usual energy gap in the other spin-direction.[58].

In a previous work several SGS compounds have been identified. Motivated by potential spintronic applications, we applied the frozen magnon method as implemented in paper I together with a classical Monte Carlo method to investigate their magnetic properties. In paper III we report the results for the five inverse-Heusler (SGS) compounds Mn_2CoAl, Ti_2MnAl, Cr_2ZnSi, Ti_2CoSi and Ti_2VAs.

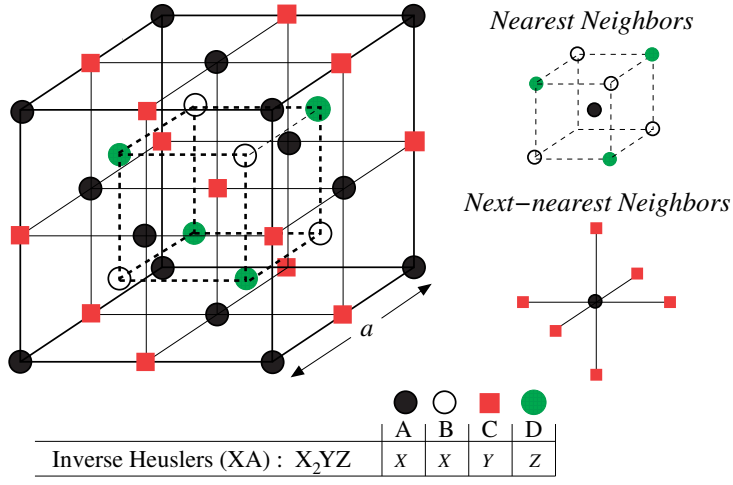

Figure 4.9. The lattice structure of inverse Heusler alloys with the chemical formula X_2YZ. X and Y are transition metal atoms (with the valence of Y larger than of X) and Z is an *sp*-element. The nearest and next-nearest neighbours of an A site are represented on the right hand-side panel.

All compounds except Ti_2CoSi are ferrimagnetic in their magnetically ordered phase. Due to gap in the minority spin channel the exchange interactions decay fast and the magnetic properties of these SGSs are determined by the nearest and next nearest neighbour exchange interactions as seen in Fig. 4.10.

Calculated exchange parameters were used to determine the temperature dependence of the magnetisation and Curie temperatures. The Tc of all the compounds are well above the room temperature (see Fig. 4.11) making them suitable for further experimental considerations. The only material among those in the study that has been synthesised to date is Mn_2CoAl. For Mn_2CoAl the temperature dependence of the magnetisation and Curie temperature are in very good agreement with available experimental data as seen in Fig. 4.11.

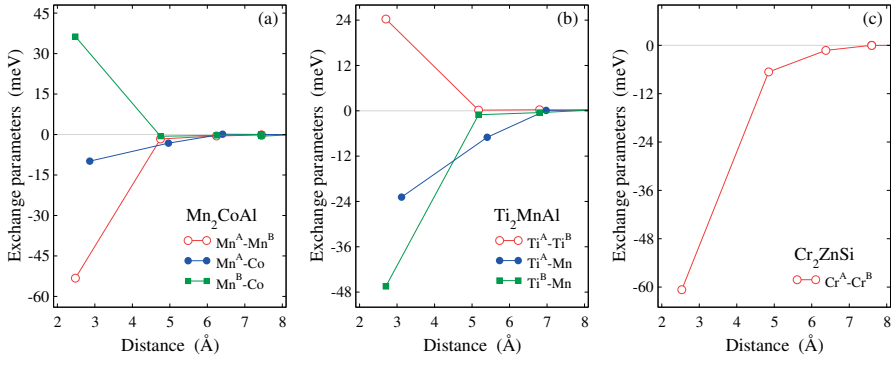

Figure 4.10. Inter-sublattice exchange interactions as a function of distance, for three different inverse Heusler alloys.

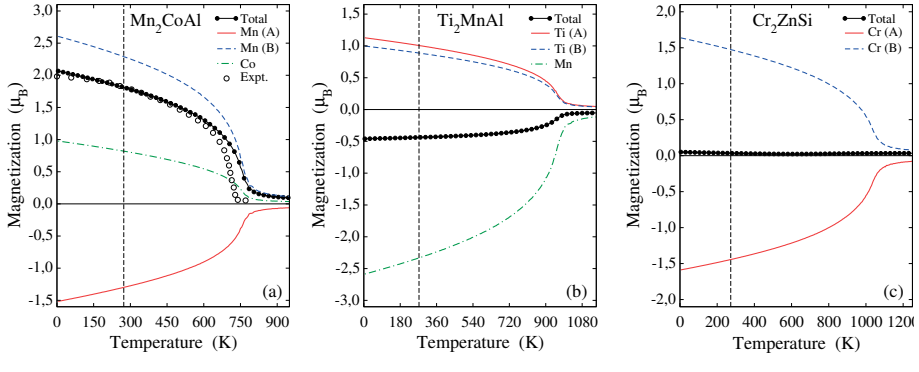

Figure 4.11. Sub-lattice magnetisation as a function of the temperature as obtained from Monte-Carlo simulations. The vertical dashed line marks the room temperature, 273 K. In the case of Mn_2CoAl we compare our calculated data with the experimental results from Ref. [59].

4.5 Constraining Fields, the MFT and Susceptibility Calculations

In paper IV we investigated the impact of the long wave length approximation in the magnetic force theorem for B2 structured FeCo and found significant differences between the non-self consistent calculations utilising the MFT and self consistent calculations. Furthermore we noted that significant improvements could be made to the non-self consistent calculations by including pre-converged constraining fields in the calculations for each spin spiral.

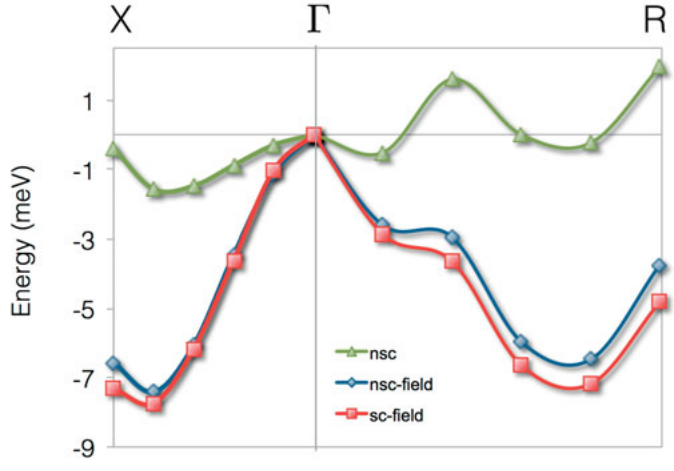

Figure 4.12. The total energy dispersion for FeCo, with a non-zero cone-angle on the Fe magnetic sub-lattice. The dispersion curves were obtained without any constraining field (green points), non-self-consistently with applied constraining field (blue points) and self-consistently with constraining fields.

In Figs. 4.12, 4.13 and 4.14 we show the results of these calculations. Here we see changes in the dispersion of spin-spirals with all different combinations of cone-angles that we normally consider in the frozen magnon method as implemented in paper I.

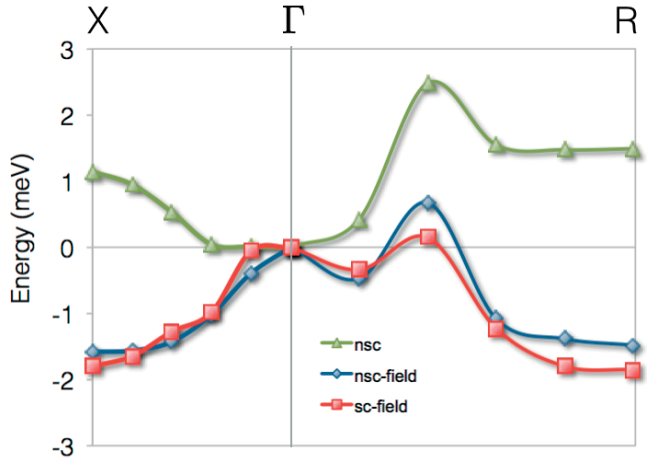

Figure 4.13. The total energy dispersion for FeCo, with a non-zero cone-angle on the Co magnetic sub-lattice.

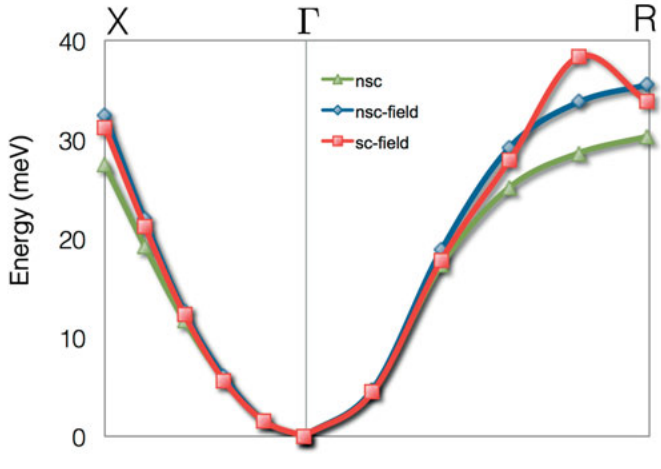

Figure 4.14. The total energy dispersion for FeCo, with a non-zero cone-angle on both Fe and Co magnetic sub-lattices.

We applied the frozen magnon method, implemented in the Elk code according to the procedure detailed in paper I, to the problem of calculating the changes in the exchange parameters due to the constraining fields. Here the frozen magnon method was modified such that the energies considered, were obtained by application of pre-converged constraining fields. The obtained exchange parameters can be seen in Figs. 4.15, 4.17 and 4.16.

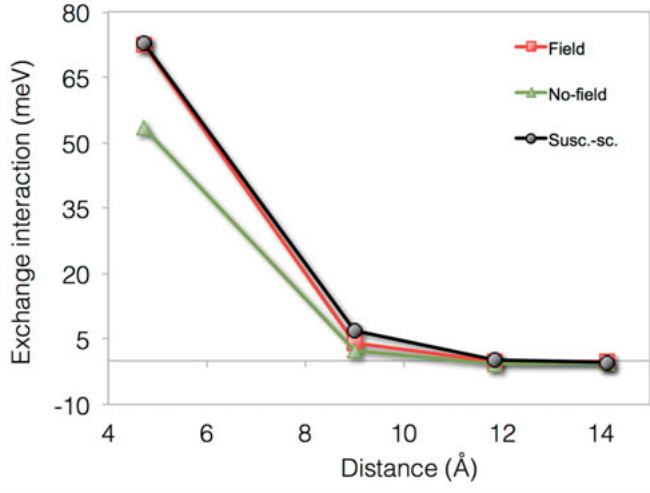

Figure 4.15. Inter-lattice (Fe-Co) exchange interactions, without any constraining field (green line), with applied constraining fields (red line) and as obtained from self-consistent susceptibility calculations (black line).

In Figs. 4.15, 4.17 and 4.16 we also include the exchange parameters generated by the newly implemented ISTS method. In this method the calculations are done self-consistently and thus the MFT is completely avoided. Since the dispersion generated with non-self consistent calculations including constraining fields correspond very well with the self-consistent dispersion, we expect the exchange parameters generated by the ISTS method to correspond well with the frozen magnon calculations that include pre-converged constraining fields. This is also the case for the inter sub lattice interactions as can be seen in Fig. 4.15. Especially noteworthy is the perfect agreement for the dominating nearest neighbour inter sub lattice interaction. However for the relatively weak intra sub lattice interactions we actually note a better agreement between the ISTS calculations and the ones obtained by the frozen magnon method without the use of constraining fields. This is contrary to expectations since the dispersion shown in Figs. 4.12, 4.13 only depends on intra-lattice interactions and we see large qualitative changes there.

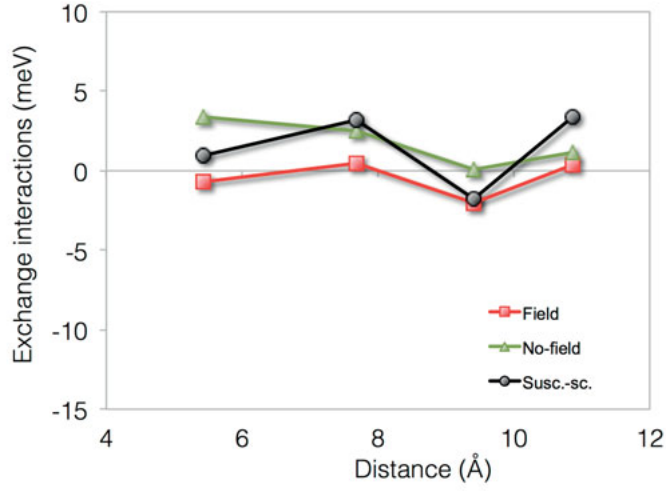

Figure 4.16. Intra-lattice (Co-Co) exchange interactions, without any constraining field (green line), with applied constraining fields (red line) and as obtained from self-consistent susceptibility calculations (black line).

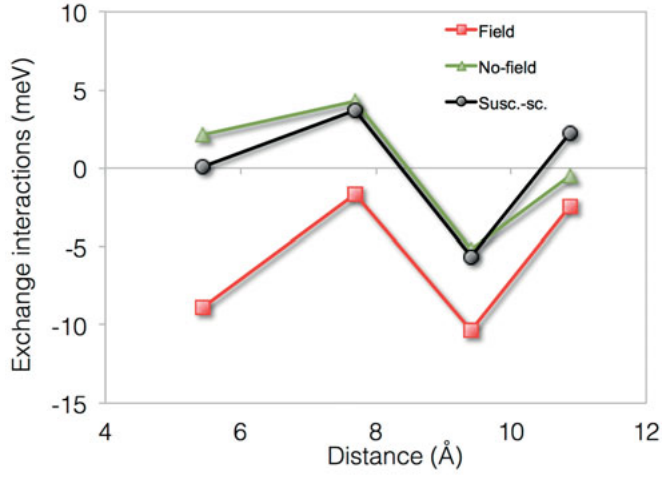

Figure 4.17. Intra-lattice (Fe-Fe) exchange interactions, without any constraining field (green line), with applied constraining fields (red line) and as obtained from self-consistent susceptibility calculations (black line).

This might be a result of the rather low number of exchange parameters used in Heisenberg model. To generate more exchange parameters we need to converge a larger set of spin-spirals in order to achieve numerical stability for a larger system of equations.

In parallel with our investigation of FeCo we applied our various methods to bcc Fe. This is a system that historically has been considered for the different correction procedures to the MFT. From the works of V. Antropov [35], P. Bruno [36], Katsnelson et al. [37], we know that corrections to the MFT typically worsen the agreement between non-self consistent and self-consistently calculated total energies for finite wave-vectors in the case of bcc Fe.

When applying pre-converged constraining fields in non-self-consistent calculations this was also the results we got. The results of the non-self-consistent calculations without fields were closer to the self-consistent total energy calculations as shown in Fig. 4.18. This imply that in this case the ISTS method should give results that are similar to the methods employing the "bare" MFT.

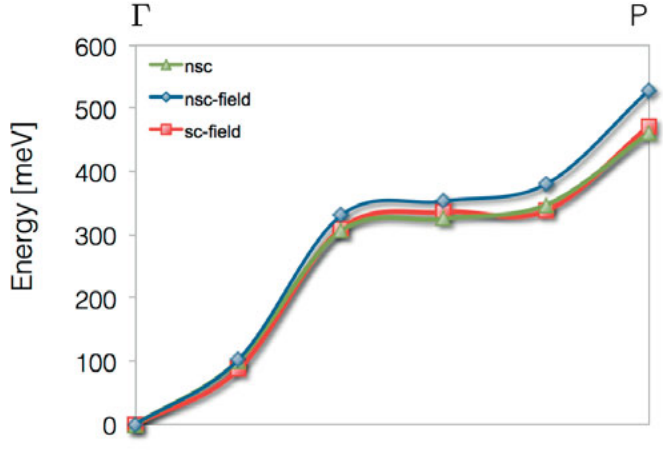

Figure 4.18. Spin-wave excitation spectrum for bcc Fe along the Γ-P symmetry line.

This was also the case as shown in Figs. 4.19 and 4.20. We obtain an almost perfect match between the exchange parameters generated by the ISTS method and exchange parameters obtained by L. Bergqvist [60] using the frozen magnon procedure and the Liechtenstein formula [34].

The comparisons in Fig. 4.20 is less exact, but still give good quantitative agreements.

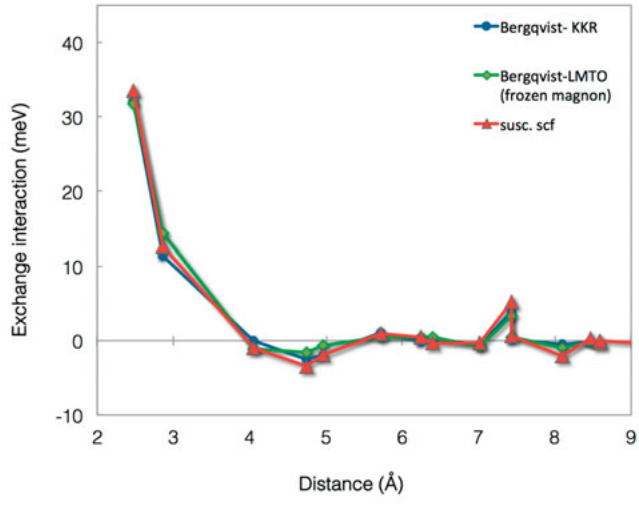

Figure 4.19. Comparison between our exchange parameters as calculated self-consistently from the static transverse susceptibility and the MFT results of L. Bergqvist [60].

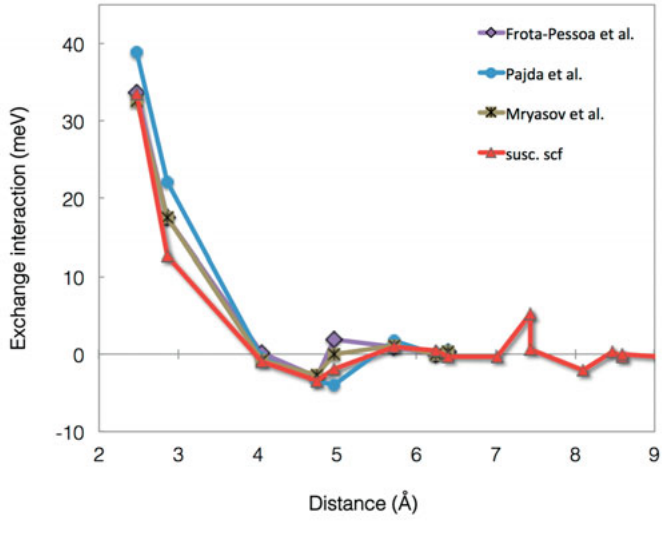

Figure 4.20. Comparison between our exchange parameters as calculated self-consistently from the static transverse susceptibility and MFT results of Pajda et al. [61], Mryasov et al. [62] and Frota-Pessoa et al. [63].

5. Perspectives and Outlook

Many questions and possibilities were created by the implementation of the inverse transverse susceptibility method into the Elk code. Most immediately there is a need to completely converge the FeCo exchange parameters calculations so that there remains no doubt about the impact of the omission of the constraining fields. We need to establish if the absence of the fields has such a large effect on this particular system, as our current calculations indicate. If so, then we might have to reconsider some of the results we obtained particularly in Paper II, and possibly in Paper III.

Furthermore it would be interesting to extend the case studies to oxides and Heusler materials since the method, due to the fact that the MFT is avoided, should be particularly effective in investigating systems with short range interactions and induced moments. Moreover, the scaling of the method with respect to the number of magnetic atoms makes it favourable to deal with relatively large multi-lattice systems (most of which are good candidates for spintronics applications).

Combining the ISTS method with more sophisticated energy functionals could further improve the accuracy and range of applications for correlated systems. Another direction could be to make an ISTS method implementation in a plane wave code to access bulk systems with larger unit cells, systems with impurities, surfaces and nano-structures.

As a next step in method development, I had the idea that there is a possibility to generalise the (already quite) generalised Bloch theorem to include a larger class of homogenous magnetic structures than the regular spin-spirals. For instance, I believe that it is possible to formulate a spin-spiral like formalism that allows for changes of the rotation axis within the unit cell, thus providing a generalisation of the frozen magnon method to complex non-collinear magnetic structures.

6. Acknowledgments

I would like to thank my supervisors Biplab Sanyal for introducing me to the field of *ab initio* calculations and for all the constructive discussions we've had over the years in the different research projects we have pursued together. In no way less I would like to thank my supervisor Marjana Ležaić for introducing me to the frozen magnon technique and the important task lending solid criticism to all the various ideas that I came up with during the years. I would also like to thank my assistant supervisors Olle Eriksson and Stefan Blügel for very helpful scientific discussions and the warm and friendly atmosphere in the groups in Uppsala and Jülich. From the group in Jülich I would also like to thank Ersoy Şaşıoğlu for an excellent collaboration, Gustav Bihlmayer for all pedagogical explanations regarding various scientific topics and help with the details of the Fleur code, Konstantin (thanks for the assistance in connection to the various DPG-meetings), Martin, Ivetta, Nicolai and Vasile and all the fellow PhD students for many great times. In Uppsala I want to mention that I greatly appreciated all the help I got from Oscar Grånäs and Lars Nordström with scientific questions and details of the Elk code. Furthermore I would like to thank Yaroslav Kvashnin for all good discussions, the efforts he spent on different small test calculations for my sake and for the excellent lunch company. A big thanks to Pablo, Marek, Karel and Marco, Iulia, Igor, Johan, Diana, Jan, Vancho, Jonathan and Alexander for many good times at Ångström and Uppsala. I would also like to thank Djalal Mirmohades for all our late night discussions about math and physics. Without those, I don't think I would have pursued a PhD in physics. I would like to take the opportunity to thank my family for all the support and encouragement over the years and finally a very professional thanks to my wife, Corina Etz.

7. Sammanfattning på svenska

Den här avhandlingen är en kombination av metodutveckling, implementering och tillämpningar. Arbetet är motiverat delvis av möjligheterna till framtida nytta i form av teknologisk utveckling och delvis av att det är roligt att tänka i nya banor. Utmaningen vi har är att beskriva magnetiska egenskaper med hög precision utifrån grundlägnade kvant mekaniska principer formulerade inom täthetsfunktionalteorin. Den frusna magnon metoden erhåller information om interaktioner inom magnetiska material genom att beräkna energin av vågliknande förändringar av riktningen av de magnetiska momenten i materialen. Denna metod implementerades i ett program baserat på täthetsfunktionalteorin på ett generellt vis som medger beräkningar av system med ett flertal magnetiska sub-gitter.

En första tillämpning av denna metod var en undersökning av hur den magnetiska ordningstemperaturen i kubiskt FeCo förändrades med en tetragonal förändring av gitterstrukturen. En dylik strukturförändring kan åstadkommas genom att bilda en film av FeCo på ett underliggande gitter med den eftersökta gitterstrukturen. Om skillnaden mellan filmens struktur och det underliggande lagret är litet kan systemet sänka sin energi genom att anpassa filmens struktur.

Motivet bakom studien var att FeCo kunde ha en tillämpning som magnetiskt lagringsmedia tack vare att energikostnaden för att förändra riktningen på de lokala magnetiska momenten är hög och de därför är stabila med avseende på temperatur och förändringar av riktningen på närliggande moment. Detta gör att man kan kan ha en hög informationstäthet på lagringsmediet. Nackdelen är dock att det är svårt att skriva till lagringsmediet. För att komma runt detta problem har HAMR metoden föreslagits där man hettar upp lagringsmediet lokalt för att lättare kunna skriva till just detta segment i lagringsmediet, vilket illustreras i Fig. 7.1.

Den magnetiska ordningstemperaturen skall därför inte vara allt för hög. I studien som presenteras i denna avhandling föreslås därför att en film av FeCo på ett underlag av Rh kan utgöra en god kandidat då ordningstemperaturen är 900 K och lägst i det intervall av strukturer som undersöktes.

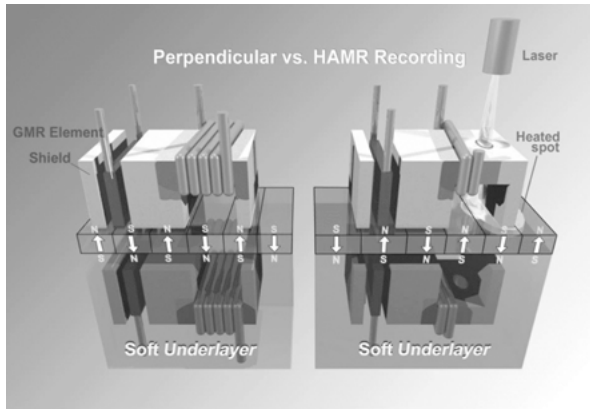

Figure 7.1. Perpendicular recording technique versus HAMR recording method. Seagate. http://www.dailytech.com/

I en andra tillämpning görs en studie av magnetiska Heusler material som har en mycket speciell elektronstruktur som gör att ledningsförmågan i materialet beror på elektronströmarnas spin. De material som studerades hade i alla fall utom ett endast studerats teoretiskt tidigare. Magnetiska egenskaper beräknades i syfte att erbjuda experimentalister möjligheten att tillverka material med lämpliga egenskaper. I det fall materialet hade tillverkats och studerats stämde de beräknade egenskaperna väldigt väl överens med experimentella resultat.

Slutligen undersökte vi det magnetiska kraftteoremet som är en approximation som är central för flertalet metoder som undersöker magnetiska interaktioner i fasta material. Den implementerade frusna magnon metoden korrigerade genom att införa magnetiska fält i beräkningarna som fixerade momentens vinklar. Det visade sig att med denna korrektion så förbättrades möjligheten att använda det magnetiska kraftteoremet avsevärt för kubiskt FeCo. Dock tillämpade vi samma korrigerade metod på bcc Fe, som är ett material där dylika korrektioner gett försämmade resultat tidigare vilket också var vad vi erhöll. Som en lösning på detta problem implementerades en metod som helt undvek det magnetiska kraftteoremet och som för en jämförbar kostnad kunde erhålla förbättrade resultat i båda fallen och därmed verkar erbjuda ett bättre tillvägagångssätt för framtida tillämpningar.

8. References

[1] P. Hohenberg and W. Kohn. Inhomogeneous electron gas. *Physical Review*, 136(3B):B864–B871, 11 1964.

[2] M. Levy. Universal variational functionals of electron densities, first-order density matrices, and natural spin-orbitals and solution of the v-representability problem. *Proc. Natl. Acad. Sci*, 76:6062–6065, 1979.

[3] W. Kohn and L. J. Sham. Self-consistent equations including exchange and correlation effects. *Phys. Rev.*, 140:A1133, 1965.

[4] Martin M R. *Electronic structure.. basic theory and practical methods* . Basic theory and practical methods. Cambridge University Press, March 2015.

[5] J. P. Perdew and Alex Zunger. Self-interaction correction to density-functional approximations for many-electron systems. *Phys. Rev. B*, 23(10):5048–5079, May 1981.

[6] John P. Perdew, Kieron Burke, and Matthias Ernzerhof. Generalized gradient approximation made simple. *Physical Review Letters*, 77(18):3865–3868, 10 1996.

[7] M Lüders, A Ernst, M Däne, Z Szotek, A Svane, D K odderitzsch, W Hergert, B L Gy orffy, and W M Temmerman. Self-interaction correction in multiple scattering theory. *Phys. Rev. B*, 71, 2005.

[8] Vladimir I Anisimov, Jan Zaanen, and Ole K Andersen. Band theory and Mott insulators: Hubbard U instead of Stoner I. *Physical Review B*, 44:943, 1991.

[9] A Petukhov, I Mazin, L Chioncel, and A Lichtenstein. Correlated metals and the LDA+U method. *Physical Review B*, 67(15):153106, April 2003.

[10] Antoine Georges and Gabriel Kotliar. Hubbard model in infinite dimensions. *Physical Review B*, 45(12):6479–6483, March 1992.

[11] Lars Hedin. New Method for Calculating the One-Particle Green's Function with Application to the Electron-Gas Problem. *Phys. Rev.*, 139(3A):A796–A823, August 1965.

[12] A. B. Shick, A. I. Liechtenstein, and W. E. Pickett. Implementation of the lda+u method using the full-potential linearized augmented plane-wave basis. *Physical Review B*, 60(15):10763–10769, 10 1999.

[13] I V Solovyev and P H Dederichs. Corrected atomic limit in the local-density approximation and the electronic structure of d impurities in Rb. *Physical Review B*, 50(23):16861–16871, December 1994.

[14] Ersoy Şaşıoğlu, Christoph Friedrich, and Stefan Blügel. Effective Coulomb interaction in transition metals from constrained random-phase approximation. *Physical Review B*, 83(12):121101, March 2011.

[15] N. W. Ashcroft and N.D. Mermin. *Solid State Physics*. Holt-Saunders Japan LTD, 1976.

[16] David Vanderbilt. Optimally smooth norm-conserving pseudopotentials. *Physical Review B*, 32(12):8412–8415, December 1985.

[17] J Slater. Wave Functions in a Periodic Potential. *Phys. Rev.*, 51(10):846–851, May 1937.
[18] D J Singh and L Nordström. *Planewaves, pseudopotentials and the LAPW method*. Springer, 2005.
[19] O.K. Andersen. Linear methods in band theory. *Phys. Rev. B*, 12(3060), 1975.
[20] E. Wimmer, H. Krakauer, M. Weinert, and A.J. Freeman. Full-potential self-consistent linearized-augmented-plane-wave method for calculating the electronic structure of molecules and surfaces: O_2 molecule. *Phys. Rev. B*, 24(864), 1981.
[21] J. Stoer. *Numerische Mathematik 1*. Springer-Verlag, 1994.
[22] E Sjöstedt, L Nordström, and D J Singh. An alternative way of linearizing the augmented plane-wave method. *Solid State Communications*, 114(1):15–20, March 2000.
[23] J Kübler, K H Hock, J Sticht, and A R Williams. Density functional theory of non-collinear magnetism. *Journal of Physics F (Metal Physics)*, 18(3):469–483, November 2000.
[24] Marjana Ležaić, Phivos Mavropoulos, Gustav Bihlmayer, and Stefan Blügel. Exchange interactions and local-moment fluctuation corrections in ferromagnets at finite temperatures based on noncollinear density-functional calculations. *Physical Review B*, 88(13):134403, October 2013.
[25] G. Rado and H. Suhl, editors. *Magnetism*. Academic Press, 1966.
[26] L.M. Sandratskii. -. *Phys. Status Solidi B*, 136(167), 1986.
[27] Ph Kurz. *Non-collinear magnetism at surfaces and in ultrathin films*. PhD thesis.
[28] O Grotheer, C Ederer, and M Fahnle. Ab initio treatment of noncollinear spin systems within the atomic-sphere approximation and beyond. *Physical Review B*, 62(9):5601–5608, September 2000.
[29] O Grotheer, C Ederer, and M Fahnle. Fast ab initio methods for the calculation of adiabatic spin wave spectra in complex systems. *Physical Review B*, 63(10):100401, February 2001.
[30] R Singer, M Fahnle, and G Bihlmayer. Constrained spin-density functional theory for excited magnetic configurations in an adiabatic approximation. *Physical Review B*, 71(21):214435, June 2005.
[31] S. V. Halilov, H. Eschrig, A. Y. Perlov, and P. M. Oppeneer. Adiabatic spin dynamics from spin-density-functional theory: Application to fe, co, and ni. *Phys. Rev. B*, 58(1):293–302, Jul 1998.
[32] Adam Jacobsson, Biplab Sanyal, Marjana Ležaić, and Stefan Blügel. Exchange parameters and adiabatic magnon energies from spin-spiral calculations. *Physical Review B*, 88(13):134427, October 2013.
[33] F. Essenberger, S. Sharma, J. K. Dewhurst, C. Bersier, F. Cricchio, L. Nordström, and E. K. U. Gross. Magnon spectrum of transition-metal oxides: Calculations including long-range magnetic interactions using the lsda+u method. *Physical Review B*, 84(17):174425–, 11 2011.
[34] A I Liechtenstein, M I Katsnelson, V P Antropov, and V A Gubanov. Local spin density functional approach to the theory of exchange interactions in ferromagnetic metals and alloys. *Journal of Magnetism and Magnetic Materials*, 67(1):65–74, 1987.

[35] V P Antropov. The exchange coupling and spin waves in metallic magnets: removal of the long-wave approximation. *Journal of Magnetism and Magnetic Materials*, 262(2):L192–L197, June 2003.

[36] P Bruno. Exchange Interaction Parameters and Adiabatic Spin-Wave Spectra of Ferromagnets: A "Renormalized Magnetic Force Theorem". *Phys. Rev. Lett.*, 90(8):087205, February 2003.

[37] M I Katsnelson and A I Lichtenstein. Magnetic susceptibility, exchange interactions and spin-wave spectra in the local spin density approximation. *Journal of Physics: Condensed Matter*, 16(41):7439–7446, October 2004.

[38] Ersoy Şaşıoğlu, Christoph Friedrich, and Stefan Blügel. Strong magnon softening in tetragonal FeCo compounds. *Physical Review B*, 87(2):020410, January 2013.

[39] Vladimir I. Anisimov, Jan Zaanen, and Ole K. Andersen. Band theory and mott insulators: Hubbard u instead of stoner i. *Physical Review B*, 44(3):943–954, 07 1991.

[40] I Solovyev and K Terakura. Effective single-particle potentials for MnO in light of interatomic magnetic interactions: Existing theories and perspectives. *Physical Review B*, 58(23):15496–15507, December 1998.

[41] O. Bengone, M. Alouani, P. Blöchl, and J. Hugel. Implementation of the projector augmented-wave lda+u method: Application to the electronic structure of nio. *Physical Review B*, 62(24):16392–16401, 12 2000.

[42] A. Rohrbach, J. Hafner, and G. Kresse. Molecular adsorption on the surface of strongly correlated transition-metal oxides: A case study for co/nio(100). *Physical Review B*, 69(7):075413–, 02 2004.

[43] Wei-Bing Zhang, Yu-Lin Hu, Ke-Li Han, and Bi-Yu Tang. Pressure dependence of exchange interactions in nio. *Physical Review B*, 74(5):054421–, 08 2006.

[44] Z. Szotek, W. M. Temmerman, and H. Winter. Application of the self-interaction correction to transition-metal oxides. *Physical Review B*, 47(7):4029–4032, 02 1993.

[45] A. Svane and O. Gunnarsson. Transition-metal oxides in the self-interaction–corrected density-functional formalism. *Physical Review Letters*, 65(9):1148–1151, 08 1990.

[46] D. Ködderitzsch, W. Hergert, W. M. Temmerman, Z. Szotek, A. Ernst, and H. Winter. Exchange interactions in nio and at the nio(100) surface. *Physical Review B*, 66(6):064434–, 08 2002.

[47] J. Kuneš, V. I. Anisimov, S. L. Skornyakov, A. V. Lukoyanov, and D. Vollhardt. Nio: Correlated band structure of a charge-transfer insulator. *Physical Review Letters*, 99(15):156404–, 10 2007.

[48] C. Franchini, V. Bayer, R. Podloucky, J. Paier, and G. Kresse. Density functional theory study of mno by a hybrid functional approach. *Physical Review B*, 72(4):045132–, 07 2005.

[49] Xiaobing Feng. Electronic structure of mno and coo from the b3lyp hybrid density functional method. *Physical Review B*, 69(15):155107–, 04 2004.

[50] Martin Schlipf, Markus Betzinger, Christoph Friedrich, Marjana Ležaić, and Stefan Blügel. Hse hybrid functional within the flapw method and its application to gdn. *Physical Review B*, 84(12):125142–, 09 2011.

[51] G Pepy. Spin waves in MnO; from 4 K to temperatures close to T_N. *Journal of*

Physics and Chemistry of Solids, 35:433, 1974.

[52] Masahumi Kohgi, Yoshikazu Ishikawa, Isao Harada, and Kazuko Motizuki. Spin waves in manganese monoxide. *Journal of the Physical Society of Japan*, 36(1):112–122, 1974.

[53] Andrew L. Goodwin, Martin T. Dove, Matthew G. Tucker, and David A. Keen. Mno spin-wave dispersion curves from neutron powder diffraction. *Physical Review B*, 75(7):075423–, 02 2007.

[54] F Yildiz, M Przybylski, X D Ma, and J Kirschner. Strong perpendicular anisotropy in Fe1-xCox alloy films epitaxially grown on mismatching Pd(001), Ir(001), and Rh(001) substrates. *Physical Review B*, 80(6):064415, August 2009.

[55] Koichi Momma and Fujio Izumi. VESTA?3for three-dimensional visualization of crystal, volumetric and morphology data. *J Appl Crystallogr*, 44(6):1272–1276, October 2011.

[56] R. A. de Groot, F. M. Mueller, P. G. van Engen, and K. H. J. Buschow. *Phys. Rev. Lett.*, 50:2024, 1983.

[57] W. E. Pickett and H. Eschrig. Half metals: from formal theory to real material issues. *J. Phys.: Condens. Matter*, 19:315203, 2007.

[58] Isaak M. Tsidilkovski. *Electron Spectrum of Gapless Semiconductors Springer Series in Solid-State Sciences*, volume 116. Springer Verlag, New York, 1996.

[59] S. Ouardi, G. H. Fecher, C. Felser, and J. Kübler. Realization of spin gapless semiconductors: the heusler compound mn_2coal. *Phys. Rev. Lett.*, 110:100401, 2013.

[60] Lars Bergqvist. *Electronic structure and statistical methods applied to nanomagnetism, diluted magnetic semiconductors and spintronics*. PhD thesis, 2005.

[61] M Pajda, J Kudrnovsky, I Turek, V Drchal, and P Bruno. Ab initio calculations of exchange interactions, spin-wave stiffness constants, and Curie temperatures of Fe, Co, and Ni. *Physical Review B*, 64(17):174402, October 2001.

[62] O N Mryasov, A J Freeman, and A I Liechtenstein. Theory of non-Heisenberg exchange: Results for localized and itinerant magnets. *Journal of Applied Physics*, 79(8):4805, 1996.

[63] Pessoa S Frota, R Muniz, and J Kudrnovsky. Exchange coupling in transition-metal ferromagnets. *Physical Review B*, 62(9):5293–5296, September 2000.

Acta Universitatis Upsaliensis

Digital Comprehensive Summaries of Uppsala Dissertations from the Faculty of Science and Technology 1236

Editor: The Dean of the Faculty of Science and Technology

A doctoral dissertation from the Faculty of Science and Technology, Uppsala University, is usually a summary of a number of papers. A few copies of the complete dissertation are kept at major Swedish research libraries, while the summary alone is distributed internationally through the series Digital Comprehensive Summaries of Uppsala Dissertations from the Faculty of Science and Technology. (Prior to January, 2005, the series was published under the title "Comprehensive Summaries of Uppsala Dissertations from the Faculty of Science and Technology".)

Distribution: publications.uu.se
urn:nbn:se:uu:diva-246766

ACTA
UNIVERSITATIS
UPSALIENSIS
UPPSALA
2015